TISSUE ENGINEERING AND REGENERATIVE MEDICINE

A Nano Approach

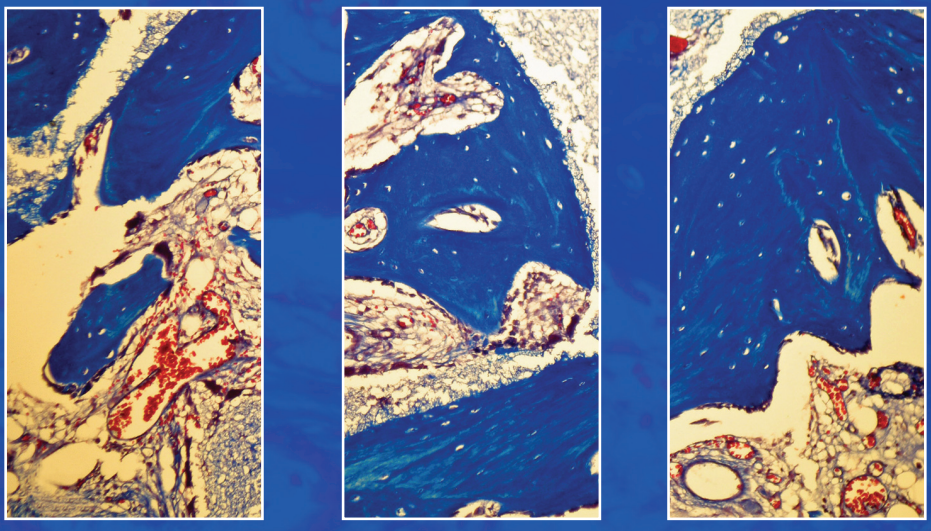

Edited by
Murugan Ramalingam • Pekka Vallittu
Ugo Ripamonti • Wan-Ju Li

CRC Press
Taylor & Francis Group

TISSUE ENGINEERING AND REGENERATIVE MEDICINE

A Nano Approach

TISSUE ENGINEERING AND REGENERATIVE MEDICINE

A Nano Approach

Edited by

Murugan Ramalingam
Pekka Vallittu
Ugo Ripamonti
Wan-Ju Li

CRC Press
Taylor & Francis Group
Boca Raton London New York

CRC Press is an imprint of the
Taylor & Francis Group, an **informa** business

CRC Press
Taylor & Francis Group
6000 Broken Sound Parkway NW, Suite 300
Boca Raton, FL 33487-2742

Version Date: 20120719

International Standard Book Number-13: 978-1-4398-8186-6 (eBook - PDF)

Visit the Taylor & Francis Web site at
http://www.taylorandfrancis.com

and the CRC Press Web site at
http://www.crcpress.com

Dedication

This book is dedicated to students, researchers and teachers who contributed to the development of tissue engineering and regenerative medicine.

Contents

Preface

Tissue engineering and regenerative medicine, including dentistry, promise to provide solutions based on integrated strategies of life science, engineering, and clinical medicine to current health challenges. Given that the field of tissue engineering and regenerative medicine is developed at a rapid pace and new findings are disclosed constantly, the state of the art of knowledge has to be continually updated. In the past several years, a number of textbooks that aim at covering current topics of tissue engineering and regenerative medicine have been published, but few of them are intended to compile all the aspects of tissue engineering and regenerative medicine and dentistry from fundamental principles to current advances and future trends. We, the editors, decided to edit a new textbook that is distinct from other available with a specific theme focusing on the utilization of nanotechnology, biomaterials science in tissue engineering, and regenerative medicine without forgetting certain important clinical aspects. We invited internationally known basic scientists, engineers, and clinicians to contribute to this book.

This book contains 24 chapters, and the topics cover the areas of nanobiomaterial and scaffold (Chapters 1–11), tissue mechanics (Chapter 12), stem cell (Chapter 13), bone tissue engineering (Chapters 14–16), cartilage tissue engineering (Chapters 17–19), controlled release (Chapters 20–22), and animal science and clinical medicine (Chapters 23 and 24). Readers will find that this book collectively bridges the gap between nanotechnology and tissue engineering and regenerative medicine to facilitate the merger of these two emerging research fields for translating laboratory discovery of tissue engineering and regenerative medicine to clinical applications through the use of nanoscale approaches.

We are grateful to all the contributors for their time and effort to deliver their chapters within a limited time frame. Without their contribution, this book could not have been completed. We also thank the publisher, CRC Press, in particular, Allison Shatkin, Amy Blalock, and Andrea Dale, for their support to publish this book on time. Finally, we hope readers will find it enjoyable to read this book to satisfy their intellectual needs.

Murugan Ramalingam
Pekka Vallittu
Ugo Ripamonti
Wan-Ju Li

Acknowledgments

The editors gratefully acknowledge all the authors who contributed to the success of the book. This book will not succeed without their insights and perspectives. We also appreciate the support and encouragement from the colleagues and students in the following departments: Centre for Stem Cell Research at the Christian Medical College in India, Faculty of Dental Surgery at the University of Strasbourg in France, World Premier International Advanced Institute for Materials Research at the Tohoku University in Japan, Turku Clinical Biomaterials Centre at the University of Turku in Finland, Bone Research Laboratory at the University of Witwatersrand in South Africa, and Musculoskeletal Biology and Regenerative Medicine Laboratory at the University of Wisconsin–Madison in the United States. Other valuable suggestions were made by anonymous referees, whom the editors would like to convey our special thanks. Our publisher, CRC Press, has been extraordinarily supportive and patient with our process. Our special thanks go to the editorial staff at CRC Press, especially Allison Shatkin, Editor of Materials Science and Chemical Engineering, and other supportive staff, who greatly amended the text format, technical corrections, and presentation style. We also wish to thank and formally acknowledge all the publishers and authors, indicated in the text and figures, who granted us permission to use their material in this book. This list is incomplete and we apologize to anyone we omitted.

Editors

Murugan Ramalingam is an Associate Professor and Scientist 'G' at the Centre for Stem Cell Research (CSCR), Department of Biotechnology, Government of India, Christian Medical College Bagayam Campus, Vellore, Tamil Nadu, India. Concurrently, he is an Adjunct Associate Professor at the Tohoku University, Sendai, Miyagi, Japan. Prior to joining the CSCR, he was an Associate Professor of Biomaterials and Tissue Engineering at the Institut National de la Santé et de la Recherche Médicale (INSERM) U977, Faculté de Chirurgie Dentaire, Université de Strasbourg, Strasbourg, France. He has worked at the WPI Advanced Institute for Materials Research, Japan, as an Assistant Professor. He has also worked at the National Institute of Standards and Technology, Gaithersburg, MD, and the National Institutes of Health, Bethesda, MD, under the U.S. National Academies Associateship program. He received his degree in the Doctor of Philosophy (Biomaterials) from the University of Madras, Chennai, India. He has also undergone training in Ethical and Policy Issues on Stem Cells from Harvard University, Cambridge, MA, and in Operations Management from the University of Illinois-Chicago. His current research interests are focused on the development of multiphase biomaterials, through conventional to nanotechnology to biomimetic approaches, cell patterning, stem cell differentiation, and tissue engineering. He is the author of over 125 publications, including peer-reviewed journal papers, conference proceedings, book chapters, authored books, edited books, and patents relevant to biomaterials and tissue engineering. He serves on the editorial boards of multiple biomaterials and tissue engineering-related journals, e.g., as the Editor-in-Chief of the *Journal of Bionanoscience* and the *Journal of Biomaterials and Tissue Engineering*. He is a recipient of Fellowships from the Council of Scientific and Industrial Research (India), Singapore Millenium Foundation (Singapore), the National Research Council (U.S.A), the National Professeur des Universités (France), and the Royal Society of Chemistry (U.K.).

Professor Pekka Vallittu has earned his degrees of certified dental technician in 1988, Doctor of Dental Surgery and Doctor of Philosophy in 1994, received Adjunct Professorship in 1995, and specialized in prosthodontics and stomatognathic physiology (European Prosthodontic Association Recognized Prosthodontist) in 2000. Presently, he is a Full Professorship of Biomaterials Science in the Faculty of Medicine, University of Turku, Turku, Finland, and works as the Dean of the Institute of Dentistry and the Director of Turku Clinical Biomaterials Centre (http://www.biomaterials.utu.fi). He is

also an Honorary Professor at the University of Hong Kong, Pokfulam, Hong Kong. His research activity on fiber-reinforced composites started from his hobby of model aircraft and has lasted for more than 25 years; first applications for fiber-reinforced composites were in dentistry, followed by active research to utilize fiber-reinforced composites as biomimetic materials, also in medicine. He has been coordinating several large research projects, for example, Nonmetallic Bioactive Fiber-Reinforced Composite Implant – research project (NEWBONE), which is funded by the European Commission and aimed at developing nonmetallic bioactive orthopedic implants. Pekka Vallittu has over 300 original research papers, 500 other papers and abstracts, and 140 granted international patents based on 17 innovations and has been awarded by Distinguished Scientist Award in Prosthodontics and Implant Research by the International Association of Dental Research.

Ugo Ripamonti is a Professor and the Director of the Bone Research Laboratory, a Research Unit of the South African Medical Research Council and the University of the Witwatersrand, Johannesburg, South Africa, within the Faculty of Health Sciences at the Medical School. He received his degrees of the Doctor of Medicine (1978) and the Doctor of Dental Surgery (1990), *cum laude*, from the University of Milan, Milan, Italy, and the Doctor of Philosophy degree in cell biology (1993) from the University of the Witwatersrand. Dr. Ripamonti is a national and an international scholar focusing on experimentation on tissue engineering of bone, tissue induction, and morphogenesis by transforming growth factor-βs and osteoinductive biomimetic matrices in preclinical and clinical contexts. He has received numerous awards, including the Marshall R. Urist Awarded Lecture at the Sixth International Conference on Bone Morphogenetic Proteins in 2006 in Dubrovnik. Dr. Ripamonti was recognized by the University of the Witwatersrand as the recipient of the prestigious Vice-Chancellor Research Award (1993) and the Distinguished Researchers Award (1995). He has published more than 200 scientific papers, including patents and book chapters for specialists.

Professor Wan-Ju Li is the Principal Investigator of the Musculoskeletal Biology and Regenerative Medicine Laboratory at the University of Wisconsin-Madison. He is also an affiliated Faculty Member in the Cellular and Molecular Biology Program, Stem Cell and Regenerative Medicine Center. His research interests include stem cell, tissue engineering, nanobiomaterial, and skeletal biology. Professor Li is a Member of the International Society for Stem Cell Research, the Orthopaedic Research Society, the Tissue Engineering International and Regenerative Medicine Society, the American Society for Cell Biology, and the American Society for Bone and Mineral Research. He has published 30 papers, 9 book chapters, and more than 60 abstracts. He holds three patents in cartilage,

intervertebral disc, and tendon/ligament applications. Professor Li has received the Fellow Award for Research Excellence from the National Institutes of Health and the Young Investigator Research Award from the North American Spine Society. He also serves in the editorial board of the American Journal of Stem Cells, the Journal of Regenerative Medicine and Tissue Engineering, the Formosan Journal of Musculoskeletal Disorders, and the Journal of Biosensors and Bioelectronics.

Contributors

Mauro Alini
AO Research Institute Davos
Davos, Switzerland

John G. Barber
Department of Orthopedics and Rehabilitation
University of Wisconsin-Madison
Madison, Wisconsin

Clark E. Barrett
Department of Materials Science and Metallurgy
University of Cambridge
Cambridge, U.K.

Serena M. Best
Department of Materials Science and Metallurgy
University of Cambridge
Cambridge, U.K.

Patrick T. Brown
Department of Orthopedics and Rehabilitation
University of Wisconsin-Madison
Madison, Wisconsin

Ruth E. Cameron
Department of Materials Science and Metallurgy
University of Cambridge
Cambridge, U.K.

Yoon N. Cho
Department of Bioengineering and Regenerative Medicine
Utah-Inha DDS and Advanced Therapeutics Research Center
Incheon, Republic of South Korea

Marcus T. Cicerone
Polymers Division
National Institute of Standards and Technology
Gaithersburg, Maryland

Meng Deng
Institute for Regenerative Engineering
University of Connecticut Health Center
Farmington, Connecticut

Dilip Dey
Aesthetic and Plastic Surgery Institute
University of California, Irvine
Irvine, California

Ivan Donati
Department of Life Sciences
University of Trieste
Trieste, Italy

David Eglin
AO Research Institute Davos
Davos, Switzerland

Elodie Faure
Department of Materials Science
Polytech Grenoble
Grenoble, France

Matthew B. Fisher
Department of Orthopedic Surgery
University of Pennsylvania
Philadelphia, Pennsylvania

Aziz Ghahary
Department of Surgery
University of British Columbia
Vancouver, British Columbia, Canada

Jyotsnendu Giri
Polymers Division
National Institute of Standards and Technology
Gaithersburg, Maryland

Sibylle Grad
AO Research Institute Davos
Davos, Switzerland

Z. S. Haidar
Department of BioEngineering
University of Utah
Salt Lake City, Utah

Andrew M. Handorf
Department of Orthopedics and Rehabilitation
University of Wisconsin-Madison
Madison, Wisconsin

Ryan Hartwell
Department of Surgery
University of British Columbia
Vancouver, British Columbia, Canada

James J. Hickman
NanoScience Technology Center
University of Central Florida
Orlando, Florida

Leena Hupa
Process Chemistry Centre
Åbo Akademi University
Turku, Finland

Roshan James
Institute for Regenerative Engineering
University of Connecticut Health Center
Farmington, Connecticut

Shaheen Jeeawoody
Department of Bioengineering
Stanford University
Stanford, California

Frank Ko
Department of Materials Engineering
University of British Columbia
Vancouver, British Columbia, Canada

Sangamesh G. Kumbar
Institute for Regenerative Engineering
University of Connecticut Health Center
Farmington, Connecticut

Kurt Lädrach
Inselspital
Bern, Switzerland

Janice H. Lai
Department of Mechanical Engineering
Stanford University
Stanford, California

Cato T. Laurencin
Institute for Regenerative Engineering
University of Connecticut Health Center
Farmington, Connecticut

Victor Leung
Department of Materials Engineering
University of British Columbia
Vancouver, British Columbia, Canada

Wan-Ju Li
Department of Orthopedics and Rehabilitation
University of Wisconsin-Madison
Madison, Wisconsin

Paula Linderbäck
Institute of Dentistry
University of Turku
Turku, Finland

Eleonora Marsich
Department of Life Sciences
University of Trieste
Trieste, Italy

Robert L. Mauck
Department of Orthopedic Surgery
University of Pennsylvania
Philadelphia, Pennsylvania

Daniel G. Miller
Excorp Medical, Inc.
St. Paul, Minnesota

Peter Molnar
Department of Zoology
University of West Hungary
Szombathely, Hungary

Debasish Mondal
Department of Clinical and Experimental Medicine
Linköping University
Linköping, Sweden

Niko Moritz
Institute of Dentistry
University of Turku
Turku, Finland

Shirley Keolebogile Motaung
Department of Orthopedic Surgery
University of California, Davis
Sacramento, California

Timo O. Närhi
Institute of Dentistry
University of Turku
Turku, Finland

Sergio Paoletti
Department of Life Sciences
University of Trieste
Trieste, Italy

Jean-Claude Petit
Faculty of Health Sciences
Medical Research Council/University of the Witwatersrand
Parktown, South Africa

Murugan Ramalingam
National Institute of Health and Medical Research UMR977
University of Strasbourg
Strasbourg, France
and
World Premier International Advanced Institute for Materials Research (WPI-AIMR)
Tohoku University
Sendai, Japan
and
Centre for Stem Cell Research
Christian Medical College Campus
Vellore, India

Anusuya Ramasubramanian
Department of Bioengineering
University of California, Berkeley
Berkeley, California

A. Hari Reddi
Department of Orthopedic Surgery
University of California, Davis
Sacramento, California

Louise Renton
Faculty of Health Sciences
Medical Research Council/University of the Witwatersrand
Parktown, South Africa

George K.B. Sándor
Regea Institute for Regenerative Medicine
University of Tampere
Tampere, Finland
and
Oral and Maxillofacial Surgery
University of Oulu
Oulu, Finland

Koteshwar N. Sridhar
Sri Research for Tissue Engineering Private Limited
Bangalore, India

Martin J. Stoddart
AO Research Institute Davos
Davos, Switzerland

Andrea Travan
Department of Life Sciences
University of Trieste
Trieste, Italy

Tuomas Waltimo
Institute of Preventive Dentistry and Oral Microbiology
University of Basel
Basel, Switzerland

Fan Yang
Department of Bioengineering
Stanford University
Stanford, California

Heejae Yang
Department of Materials Engineering
University of British Columbia
Vancouver, British Columbia, Canada

Nicola U. Zitzmann
School of Dental Medicine
University of Basel
Basel, Switzerland

1 Biostable Composite Biomaterials in Medical Applications

Pekka K. Vallittu

CONTENTS

1.1 INTRODUCTION

Replacement of damaged tissues by medical or dental biomaterials after an injury or disease requires certain properties from biomaterials. There is a trend to utilize non-metallic biomaterials, polymers, ceramics, and composites rather than metals, although metals are durable and can withstand physiological stress well. However, metals and devices made out of metals do not fulfill biomechanical requirements (isoelasticity) of bone and tooth substance, resulting in insufficient (stress-shielding) or overloading situations, and involve potential cytotoxicity arising from metal ion liberation and harmful corrosion products [1,2]. In addition, metallic objects interfere with medical diagnostics by magnetic resonance imaging (MRI) [3–5]. There are a number of polymer-based composites that are often utilized in tissue engineering and biodegradable scaffolds and drug-releasing systems and also as actual reconstructive devices [6,7]. Consequently, medical biomaterials can be classified according to their use as *reconstructive* and *regenerative* biomaterials—the first one having long-term durability, and the latter one to be typically resorbable in nature. One new group of engineering materials that has started to be utilized in reconstructive medical implants is fiber-reinforced composites (FRCs). They are presently biostable, although bioresorbable FRCs are to be developed

and known for high strength and bone-like mechanical behavior [8–13]. A number of studies have been conducted to demonstrate the biomechanical suitability and biocompatibility of FRCs to be used as reconstructive medical implant material and prosthodontic and restorative material in dentistry. These aspects are reported and discussed.

1.2 MATERIALS

1.2.1 Resin Matrices

Resins that are used in medical and dental FRCs are thermoplastics, thermosets, or their combinations in the form of semiinterpenetrating polymer networks (semi-IPNs).

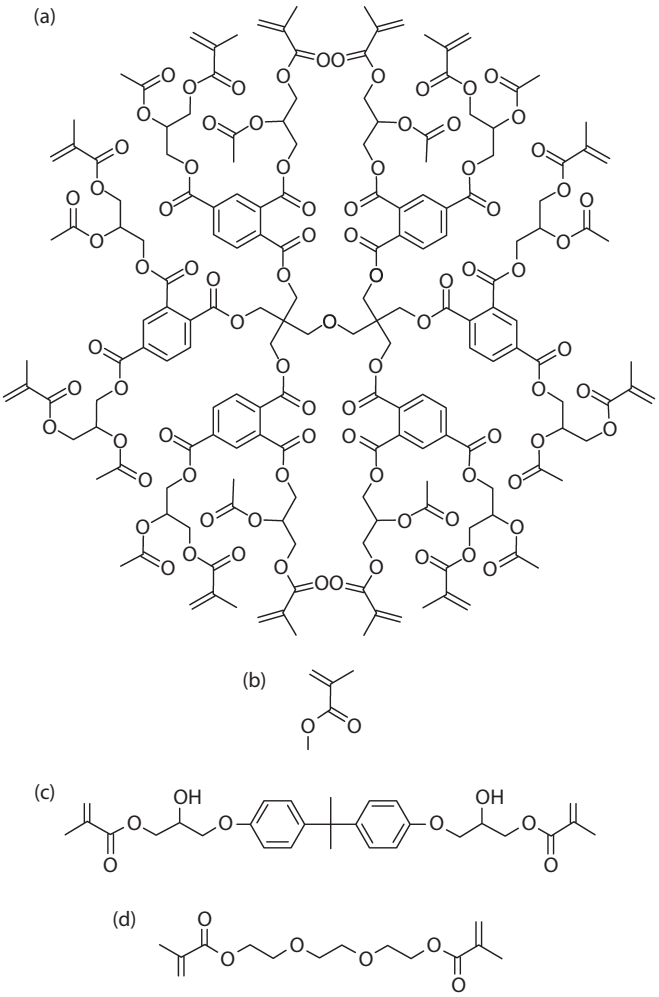

FIGURE 1.1 Chemical structures of monomers used in matrices of composites. (a) Methacrylated dendrimer. (b) Methylmethacrylate. (c) Bis-GMA. (d) TEGDMA.

Examples of thermoplastics are polyethylene (PE), polyetheretherketone (PEEK), polyacetal, and polyurethane. Examples of thermosets that are utilized as biomaterials are epoxies and bis-glycidyl-A-dimethacrylate (Bis-GMA), bis-glycidyl ethylmethacrylate (Bis-EMA), and triethylene glycol dimethacrylate (TEGDMA). Methacrylated dendrimers have also been tested as a resin matrix for FRCs (Figure 1.1).

Thermosets exhibit high cross-linking density, which makes them stiffer and more fragile. Mechanical properties of biostable polymers are presented in Table 1.1.

Resin matrix for the reinforcing fibers is cured in contact to the glass fibers (thermosets and semi-IPN matrices) or melted or dissolved for impregnation of fibers (thermoplastics). By sizing the hydroxyl-covered glass fibers with silane and by using a monomer resin system of thermoset or semi-IPN polymer, the adhesion of polymer matrix to fibers is based on chemical reaction and physical attachment.

The polymerization reaction of monomer systems of thermoset and semi-IPN polymers is based on free radical (vinyl) polymerization. Initiation of the polymerization is made by blue light radiation or by increasing the temperature [16]. Normally, the light-initiated polymerization is based on the activation of initiator camphorquinone

TABLE 1.1
Mechanical Properties of Typical Bulk Biomaterials and Hard Tissues

Material	Modulus (GPa)	Tensile Strength (MPa)
Polymers		
Polyethylene	0.88	35
Polyetheretherketone	8.3	139
Polyacetal	2.1	67
Polyurethane	0.02	35
Polymethylmethacarylate	2.5	59
Polytetrafluoroethylene	0.5	28
Polyethylene terepthalate	2.85	61
Poly(bis-glycidyl-A-dimethacrylate)-poly(triethylene glycol dimethacrylate)	8.0	52
Metals		
Stainless steel	190	586
Cobalt–chromium alloy	210	1085
Titanium alloy	116	965
Hard Tissues		
Cortical bone (longitudinal)	17.7	133
Cortical bone (transversal)	12.8	52
Cancellous bone	0.4	7.4
Enamel	84.3	10
Dentine	11.0	39.3

Source: S. Ramakrishna et al., *Composites and Technology* 61 (2001); E. Asmussen and A. Peutzfeldt. *Dental Materials* 14 (1998) 51.

and activator amine. Heat-induced polymerization is based on activations of benzoyl peroxide initiator by increased temperature. If the monomer system is aimed to be cured without temperature increase or light radiation, an activator of tertiary amine is increased to the initiator system. Examples of these autopolymerizing resins are polymethylmethacarylate (PMMA) and pBis-GMA–TEGDMA bone cements and PMMA denture rebasing and repair resins [17,18]. Autopolymerization and light curing polymerization result in a polymer with a lower degree of monomer conversion than that of the polymer cured by increased temperature. Lower monomer conversion also increases the quantity of leachable residual monomers and thus reduces the biocompatibility of the polymer [19]. Light-cured polymers can be postcured by heat after initial curing, which considerably increases the degree of monomer conversion, reduces the quantity of residual monomers, and improves biocompatibility [20–22]. Optimal postcuring temperature is close to the glass transition temperature where there is enough thermal energy in the system to create free volume, which enables unreacted carbon–carbon double bonds to form free radicals and react with each other.

1.2.2 Fillers

Fillers that have been used in biostable polymer composites are particulate fillers of fibers. Nonresorbable and hydrolytically stable particulate fillers are used in dental filling composites, which have been in clinical use since the 1950s [23]. Since then, after many significant material improvements, restorative composite resins still suffer from two key shortcomings: deficiencies of mechanical strength and high polymerization shrinkage. Resin matrices of filling composites are dimethacrylates (Bis-GMA–TEGDMA, Bis-EMA–TEGDMA, and urethane dimethacrylate), which are polymerized by light initiation. Improvements in silanation and filler composition have led to better adhesion of fillers to the polymer matrix. Filler technology has led to the development of composite resins characterized by containing zirconia or silica nanoparticle filler of approximately 25 nm in size and nanoaggregates of approximately 75 nm in size, which improves polishability and wear resistance of the composite [24]. However, the addition of nanofillers up to 30 wt% to the microfilled composite resin decreased the degree of monomer conversion [25].

Particulate fillers have also been tested to improve the osteoconductivity of bone cements. Biodegradable particulate fillers of hydroxyapatite and bioactive glass (BAG) in the autopolymerizing PMMA matrix were preclinically studied by animal experiments [26]. By histological analysis, it was found that bone contact was observed only when BAG or hydroxyapatite was present as exposed. Fibrous tissue was found on the surface of PMMA. BAG was better able to withstand the detrimental effect of PMMA than hydroxyapatite. Hydroxyapatite has also been incorporated into the PE matrix [2]. Besides biodegradable hydroxyapatite fillers and BAG fillers, tricalcium phosphate has been added to the polymers to improve osteoconductivity. Particulate fillers, regardless of their biostability or biodegradability or their good adhesion to the polymer matrix, have limited influence to the physical properties of the composite. Thus, they cannot be utilized in load-bearing applications where high-bending, shear, or torsional stresses occur.

FRCs are reputed for their high mechanical properties. The action of reinforcing fibers is to arrest propagating cracks in the polymer matrix and reinforce the composite. FRCs is a class of materials in which the basic properties of polymers are given mechanical reinforcement by the addition of fibrous materials such as glass, carbon/graphite, ultra high molecular weight PE, or aramid fibers. The optimum properties of a reinforced resin cannot be obtained, unless there is an effective bond between the two phases. Other factors with considerable influence on the physical properties of FRCs are impregnation of the fibers with the resin matrix, the quantity of reinforcing fibers, and the orientation of the fibers [27]. Fibers that are suitable to be used in medical and dental composites are glass fibers that have been silanized for good adhesion to the polymer matrix. Adhesion has been obtained by covalent bonding of dimethacrylate monomers to the silanated surface of glass fibers during polymerization (Figure 1.2) [28]. Carbon/Graphite fibers have been utilized as medical FRCs with thermoplastic PEEK matrix. Ultra high molecular weight PE fibers lack adequate bonding to the resin matrix, and therefore, their reinforcing effect is modest.

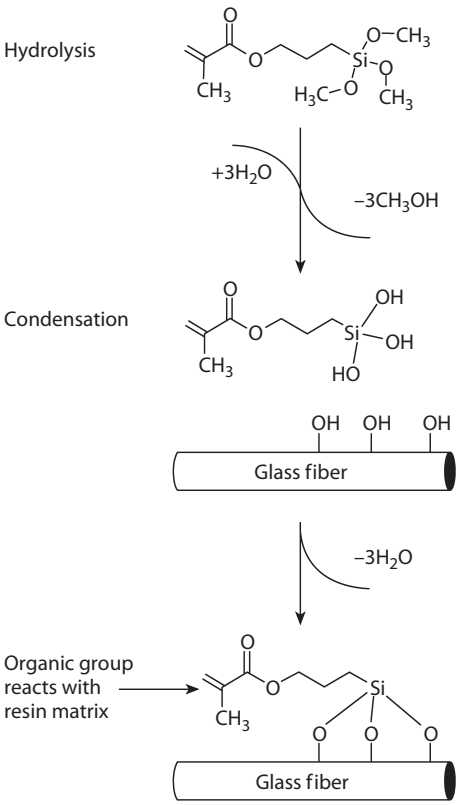

FIGURE 1.2 Schematic of the adhesion of resin matrix to the surface of silanated glass fibers. (Modified from Puska, M. et al., Evaluation of bis-GMA/MMA resin adhesion to silica-coated and silanized titanium, *Adhesion Aspects in Dentistry*, VSP, Leiden, 2009, p. 147.)

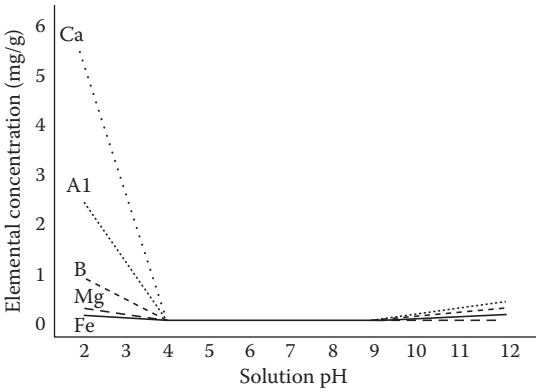

FIGURE 1.3 Stability of E-glass fibers in solutions of different pH values.

1.2.3 Hydrolytic Stability

The long-term success of reconstructive composite materials in biological environments such as in the oral cavity or insides of tissues depends on the hydrolytic stability of the composite. Hydrolytic stability is dependent on the stability of polymer matrix, fillers, and the interface between the fillers and the polymer matrix. In earlier times, dental filling composites failed, because the glass filler particles contained considerable quantities of earth alkali oxides, which were prone to leaching in the presence of water. Once the filler composition was improved to withstand the effects of water, the next weak point was the silane-promoted adhesion between the glass and the polymer matrix. Improvement of the hydrolytic stability of the interface was found to relate to the curing temperature of the silane on the glass surface. Present particulate filling composites and glass FRCs exhibit good long-term hydrolytic stability that is based on the stability of polymer matrix, fillers and fibers, and their interface [10,29–31]. It is known that good-quality and surface-purified E-glass fibers itself exhibit stability in pH values between 4 and 10 (Figure 1.3) [32].

1.3 MATERIAL PROPERTIES

1.3.1 Direction Dependency

Particulate filler composites demonstrate isotropic physical, thermal, and optical properties, whereas FRCs are either isotropic, anisotropic, or orthotropic. Thus, FRCs allow materials designing to obtain biomechanically anisotropic medical and dental devices that correspond to the behavior of bone or tooth, which are known by their anisotropic nature in terms of collagen fibril and osteon orientation (Figure 1.4) [33]. The anisotropic nature is for the optimization of mechanical load bearing of bone structures and to avoid excessive peak stresses. There is an intimate relationship between the forces acting upon bone-and-bone structure. On the topic of bone structure and bone loading, there are descriptions by Bourgery and Bell from 1832 to 1834 [34,35]. It is surprising that the utilization of this information, which is often

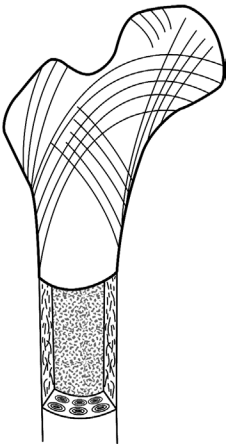

FIGURE 1.4 Anisotropic structure of bone from the level of collagen fibrils to structures of osteons can be mimicked and reconstructed by the use of fiber-reinforced composites.

called Wolff's law [36], has not been made by implant manufacturers. One reason could be in the use of isotropic metallic implants, which from the material basis, do not allow and require tailoring the biomechanical properties of the implant.

Present knowledge of biomechanical properties of FRCs, especially glass FRCs, shows good biomechanical match of FRC implants to that of bone. Studies by finite element modeling (FEM) demonstrate the stress at the bone around FRC implants to be more even than with metal implants [37]. This has also been verified by mechanical tests and animal experiments, which revealed better attachment of an FRC implant to surrounding bone-like material than what can be obtained with titanium implants [9,38]. For the optimization of the load-bearing capacity of an FRC device, the direction of load and stress needs to be known, and the fiber direction should be oriented to carry the stress. Reinforcing the efficiency of fibers is defined as Krenchel's factor—a theoretical maximum reinforcing effect that can be obtained with certain fiber orientation (Figure 1.5) [39]. Thus, the strength of FRCs is largely

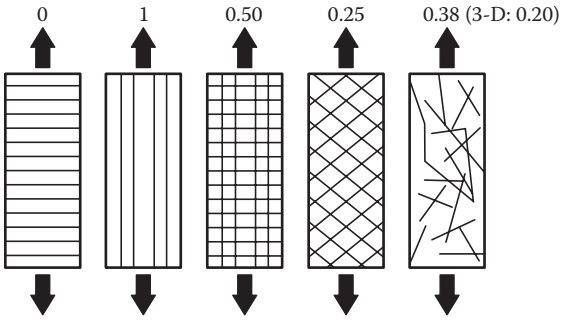

FIGURE 1.5 Reinforcing efficiency (percentage) of fibers against the direction of tensile force (arrows).

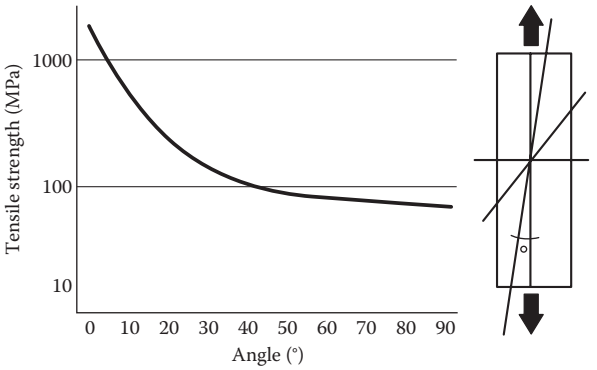

FIGURE 1.6 Alignment of reinforcing fibers against the direction of tensile force (arrow) considerably influence reinforcing effect by fibers.

dependent on the fiber direction, and the efficiency of the fiber reinforcement varies in FRC laminates with different fiber orientations (Figure 1.6) [39]. The continuous unidirectional fibers give the highest strength and modulus of elasticity for the FRCs, but the property is available only in the direction of stress equal to that of the direction of the fibers. The anisotropic behavior of unidirectional FRCs can also be seen in other properties such as thermal expansion or polymerization shrinkage [40,41].

1.3.2 Mechanical Strength

The static strength (ultimate flexural strength) of the FRCs is dependent on the fiber quantity to the level of approximately 70 vol%. A high-quality glass FRC material with high fiber quantity provides high flexural bending properties (with E-glass up to 1250 MPa; Figure 1.7) [42,43]. A positive correlation exists between the water sorption of polymer matrix and the reduction of flexural properties. For instance, the high water sorption of polyamide (nylon) matrix causes reduction of over 50% in the

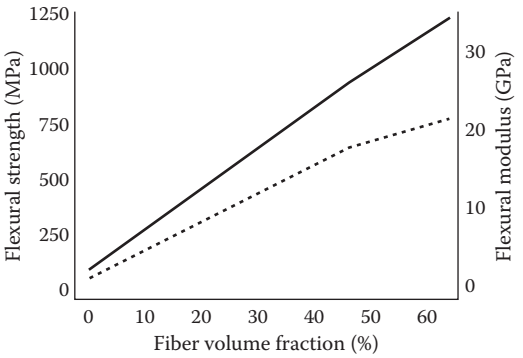

FIGURE 1.7 Flexural strength (solid line) and flexural modulus (dotted line) of unidirectional FRCs plotted against fiber volume fraction.

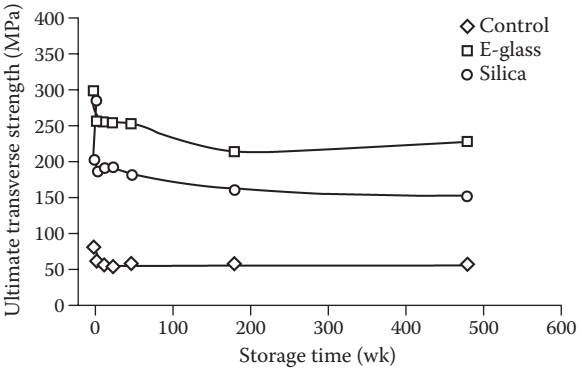

FIGURE 1.8 Flexural strength of unidirectional E-glass–PMMA, silica glass–PMMA FRCs, and plain PMMA (control) plotted against storage time in water at 37°C up to 10 years.

strength of FRCs. The reduction of the flexural properties was reversible (i.e., dehydration of the FRCs recovered the mechanical properties) [44]. Water sorption of the polymer matrix reduces the strength and modulus of elasticity of the FRCs with the semi-IPN polymer matrix of pBis-GMA–PMMA by approximately 15% within 30 days of water storage time at 37°C [44]. No significant reduction of flexural strength and modulus, even in long-term water storage (up to 10 years), occurred (Figure 1.8) [29,30].

Several studies have dealt with the strength of FRCs, which may have shown misleading values of the material strength. Testing of specimens of small dimensions, such as dental root canal posts used for anchoring crowns, can lead to incorrect results in megapascals. It is known that the commonly used mathematical formulas for calculating the flexural strength and modulus of elasticity of test specimens are dependent on the diameter (height) of the specimen and span length of the test setup for a three-point bending test [45]. With a constant span length, thinner specimens reveal higher flexural strength and modulus of elasticity values than those obtained with specimens of the same material but of a larger dimension. Thus, only the strength values of specimens of exactly the same diameter and span length, as well as crosshead speed, in the test setup are comparable. In biomedical applications, there is a need to compare different material properties such as the strength and modulus of elasticity and the load-bearing capacity and structural stiffness of the device. Clinically, the latter is more important.

1.4 BIOCOMPATIBILITY

The biocompatibility of biostable composites relates to the biocompatibility of polymer matrices, reinforcing particulates and fibers, and their combination. Biocompatibility indicates the biological performance of materials in terms of structural and surface compatibility [46,47]. Structural compatibility refers to the biomechanical properties of the implant material, such as the modulus of elasticity and strength, implant design (i.e., stiffness—a product of elastic modulus and seconds

moment of area), and optimal load transmission at the implant tissue interface (minimum interfacial strain mismatch and load transfer) [14]. Metals and ceramics have at least 10–20 times higher elastic modulus than hard tissues, and therefore, one of the major problems in orthopedic surgery has been the mismatch of stiffness between the bone and metallic implant. Thus, the bone is insufficiently loaded compared to the implants, and this condition is called stress shielding [14]. Stress shielding affects bone remodeling and healing, leading to increased bone atrophy [48]. Utilization of biomechanical properties of FRCs can overcome the aforementioned biomechanical problems, because FRC materials simultaneously exhibit bone-like modulus of elasticity and high strength. An additional merit of FRCs is that, by controlling the volume fraction and arrangement of the fibers, the properties and designs can be varied and tailored to suit the mechanical and physiological conditions of the host tissues. By arranging fibers, the FRCs can mimic natural anisotropic tissues, which depend on the structural arrangements of its components of collagen, elastin, and hydroxyapatite. By selecting FRCs for implant material, interfacial stress and strain between implant and bone can be transferred more evenly than with titanium implants [37]. The biocompatibility of using FRCs over metals includes the absence of corrosion and fatigue failures and the release of metal ions and metal nanoparticles, which may cause loosening of the implant. In the case of composite implants, tribological properties of composites and fixation devices should be optimized to eliminate the potential risk of debris formation from the composite implants.

The biocompatibility of FRC implants is basically related to the biocompatibility of its major components of polymer matrix and reinforcing fibers. Thermoset polymer FRCs have been made of epoxy polymers and of dimethacrylate polymers. The use of epoxy polymer has been criticized due to the potential toxic and sensitizing (allergic) effects of its monomers, which are present as residuals in the FRCs [49,50]. On the other hand, thermoset polymers made of dimethacrylate monomer systems of Bis-GMA and TEGDMA monomers have shown good biocompatibility after polymerization at elevated temperatures and not in the presence of oxygen (Figure 1.9) [22,51–53].

Thermoset polymers provide the chemical bonding of polymer matrix to glass fibers or other OH-covered substrate through silane coupling agents. Chemical bonding cannot be obtained by the thermal molding of thermoplastic polymers of polymer matrix for FRCs [54–56]. In thermoplastic polymer matrix FRCs, which have been processed by thermal plasticization and molding, only physical attachment of the polymer matrix to the surface of fibers occurs, whereas the polymerization of the monomer system of the thermoset resins in contact to the silanized glass fibers results in covalent and hydrogen bonding of the polymer matrix to the reinforcing fibers. Covalent bonding of polymer matrix to fibers is desired for the long-term stability of FRCs in a biological environment.

Biological testing of glass FRCs by cell cultures and animal testing has shown materials biocompatibility. Cell culture studies by fibroblasts with E-glass fibers without resin matrix have shown no signs of cytotoxicity, as it has been also demonstrated with fibroblasts by agar diffusion cytotoxicity test [57,58]. By using osteoblasts, no signs of toxic reactions of the material can be found either [59]. Rat bone marrow-derived osteoblast-like cells were harvested and cultured on experimental

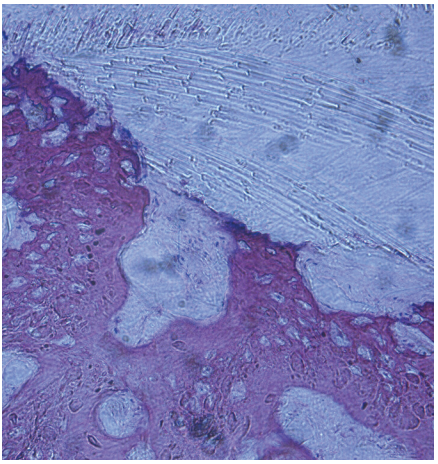

FIGURE 1.9 Histological image of E-glass FRCs showing good biological response of bone to contact of implant.

FRC material plates and on commercially pure titanium plates (control) for 21 days [60]. The materials' surfaces were characterized by roughness testing and scanning electron microscopy. Cell growth and differentiation kinetics were subsequently investigated by evaluating proliferation, alkaline phosphatase (ALP) activity, osteocalcin (OC), and bone sialoprotein (BSP) production. The maximal ALP activities on FRCs and titanium were observed after 3 weeks. The expression of osteoblastic markers (OC, BSP) indicates that the fastest osteogenic differentiation takes place on FRCs after 7 days. In contrast, a slower differentiation process was observed on titanium than on FRCs, as confirmed by the increased mRNA expression of OC and BSP. It was concluded that the proliferation and maturation of osteoblast-like cells on FRCs appears to be comparable to titanium. The presence of BAG enhances cell maturation.

A number of animal experiments have been carried out to show biological responses to E-glass FRCs. In many experimental FRC materials, there have been additional BAG particulates on the surface of the FRC implant. BAGs are synthetic resorbable biocompatible osteoconductive bone substitutes with bone bonding capacity and antibacterial and angiogenesis-promoting properties [61–68]. FRC–BAG implants have been tested by animal tests for head-and-neck applications and for orthopedics and oral implantology. Head-and-neck applications have been preclinically tested with a calvarial critical size defect model in rabbits [51,52]. Between FRC laminates of the FRC implant, there were particulates of BAG for improving osteoconductivity, angiogenesis, and antimicrobial properties. FRCs have the potential for use as load-bearing orthopedic implants if the high strength and elastic modulus of the FRC implant can be matched with local requirements. An animal study was carried out to test the *in vivo* performance of novel FRC implants made of unidirectional glass fibers (E-glass fibers in pBis-GMA–pTEGDMA polymeric matrix) [69]. The implant surface was covered with BAG granules. Control implants

were made of surface-roughened titanium. Stress-shielding effects of the implants were predicted by FEM. Surgical stabilization of bone metastasis in the subtrochanteric region of the femur was simulated in rabbits. An oblong subtrochanteric defect of a standardized size (reducing the torsional strength of the bones approximately by 66%) was created, and an intramedullary implant made of titanium or the FRC composite was inserted. The contralateral femur served as the intact control. At 12 weeks of healing, the femurs were harvested and analyzed by radiography, torsional testing, microcomputerized tomography imaging, and hard-tissue histology. The functional recovery was unremarkable in both groups, although the final analysis revealed two healed undisplaced peri-implant fractures in the group of FRC implants. FEM studies demonstrated differences in stress-shielding effects of the titanium and FRC implants, but the expected biological consequences did not become evident during the follow-up time of the animal study. Biomechanical testing of the retrieved femurs showed no significant differences between the groups. The torsional strength of the fixed bones had returned the level of contralateral intact femurs. Both implants showed ongrowth of intramedullary new bone. No adverse tissue reactions were observed.

Oral implant research has also utilized E-glass fibers in a pBis-GMA–pTEGDMA polymeric matrix system. Aside from FRCs' adequate biomechanical strength, the studies have also shown FRCs' biocompatibility in bone to be comparable to that of titanium after 4 and 12 weeks. The addition of BAG to the implant increased osteogenesis and bone maturation [70,71].

1.5 CLINICAL USE

Biostable composite implants have been used as bone plates with screw fixation made of carbon FRCs and PEEK resin matrix. Tests have also been conducted to use glass FRCs/PEEK as intramedullary nail and in spine fusions [14]. Traditional skull and facial bone reconstructions, for example, in cranioplasties are based on using hard tissues (bone grafts), which typically causes donor site morbidity. Metallic implants have been used alone or in combination with bone or hydroxyapatite cement in cranial bone reconstructions. Although these materials are readily available for immediate application, they all require preparation, adaptation, contouring into defect, and later on, resistance to traumatic insults is uncertain. In addition, metallic implants cause problems in medical imaging by X-rays or by MRI. The clinical outcome of treatments of cranioplasties showed that the most often used material is autogenous bone graft, but more than one-third of the treatments are primarily treated with artificial materials. Of all treatments, almost one-fourth are complicated, and infections and material exposure are the most critical complications [72]. Of the artificial materials, hydroxyapatatite cement was associated with the worst results, and bone grafts showed a high grade of partial resorption, which required further surgery for correction. Complications related to the exposure of the implant are related to immunoguided delayed inflammatory reactions that lead to thinning of the skin. Secondary operations for repair are difficult in these cases. Comparison of PMMA and bone grafts has also been undertaken by other researchers [73], demonstrating the exposure of PMMA and secondary infection to be the complications for PMMA.

Because PMMA is one of the most widely used alloplastic material in surgery, it has also been used as a matrix polymer for *ex vivo*–produced biostable composite implants. Because PMMA is polymerized *in situ*, the amount of the exotherm and residual monomers may cause even severe clinical problems, which lead to foreign body reaction [74,75]. To overcome these problems, patient-specific skull bone implants based on patient's preoperative three-dimensional model have started to be produced. The first-generation implants were made of PMMA that has been polymerized *ex vivo* to receive an optimal degree of monomer conversion and, thus, the lowest possible amount of residual monomers [76]. PMMA implants were coated BAG particles. By clinical and radiological follow-ups, it was demonstrated that the implants performed well 24 months postoperatively. Through computerized tomography and positron emission tomography, new bone formation was found on the surface, which had been modified by BAG. No periprosthetic infections have been supported by the *in vitro* and clinical findings of the antimicrobial properties of BAG. Based on the clinical experiences by PMMA implants, further improvements in terms of allowing new bone formation to occur faster and to have thinner margins for the implants were made by introducing glass FRC–BAG implants for a clinical trial. The FRC–BAG implants are made of load-bearing laminate and scaffold, which absorbs blood and patient's own substances (cells, growth factors, and signaling molecules) for bone formation in the scaffold (Figure 1.10). The design of the implant enables the use of nonmetallic patient-specific implants and scaffolds in tissue-engineering approaches in replacing tissues. The FRC–BAG implants have been in preliminary clinical testing since 2007 without any kinds of complications or infections [77], and they show high potential for replacing the present bulk material implants made of metals and bulk polymers. Further developments of nonmetallic biostable implants will likely be made by adding bioactive substances and drugs to the implant to be released locally in the body.

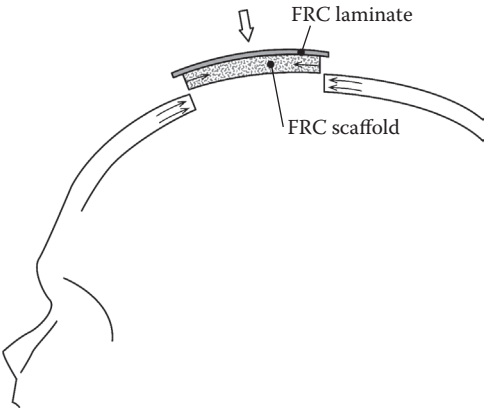

FIGURE 1.10 Schematic of the design of FRC implants for skull bone defects. The implant is having a load-bearing phase (FRC laminate) and a porous phase (FRC scaffold) into which the bone is growing.

1.6 CONCLUSION

Current needs from the biomechanical and medical imaging perspective, as well as the concern for potential harm from released metal nanoparticles and ions, have led to the development of biostable composite implants. In applications where large defects are repaired or the implant will be heavily loaded, the most suitable material alternative seems to be FRCs. FRCs made of glass fibers and dimethacrylate matrix have shown good biocompatibility, and the FRC implants have started to be tested in clinical studies with encouraging preliminary results.

REFERENCES

1. J.B. Park and R.S. Lakes. 1992. *Biomaterials: An Introduction*. New York: Plenum Press.
2. W. Bonfield, M. Grynpas, A.E. Tully, J. Bowman, and J. Abram. Hydroxyapatite reinforced polyethylene—A mechanically compatible implant material for bone replacement. *Biomaterials* 2 (1981) 185.
3. F.G. Shellock. Metallic neurosurgical implants: Evaluation of magnetic field interactions, heating, and artifacts at 1.5-tesla. *Journal of Magnetic Resonance Imaging* 14 (2001) 295.
4. A.M. Sawyer-Glover and F.G. Shellock. Pre-MRI procedure screening: Recommendations and safety considerations for biomedical implants and devices. *Journal of Magnetic Resonance Imaging* 12 (2001) 92.
5. F.G. Shellock. Biomedical implants and devices: Assessment of magnetic field interactions with a 3.0-tesla MR system. *Journal of Magnetic Resonance Imaging* 16 (2002) 721.
6. S.J. Holland, B.J. Tighe, and P.L.J. Goud. Polymers for biodegradable medical devices—Part 1: The potential of polyesters as controlled macromolecular release systems. *Controlled Release* 4 (1986) 155.
7. J.C. Middleton and A.J. Tipton. Synthetic biodegradable polymers as orthopaedic devices. *Biomaterials* 21 (2000) 2335.
8. P.K. Vallittu. The effect of glass fiber reinforcement on the fracture resistance of a provisional fixed partial denture. *Journal of Prosthetic Dentistry* 79 (1998) 125.
9. R.H. Mattila, M. Puska, L.V.J. Lassila, and P.K. Vallittu. Fiber-reinforced composite implant: *In vitro* interfacial failure mechanics and residual monomer analysis. *Journal of Materials Science: Materials in Medicine* 41 (2006) 4321.
10. S. Bouillaguet, A. Schutt, P. Alander, P.K. Vallittu, P. Schwaller, G. Buerki, J. Michler, M. Cattani-Lorente, and I. Krejci. Hydrothermal and mechanical stresses degrade fiber–matrix interfacial bond strength in dental fiber-reinforced composites. *Journal of Biomedical Materials Research, Part B: Applied Biomaterials* 76 (2006) 98.
11. A.M. Ballo, L.V.J. Lassila, T. Närhi, and P.K. Vallittu. *In vitro* mechanical testing of glass fiber-reinforced composite used as dental implant. *Journal of Contemporary Dental Practice* 9 (2008) 41.
12. D.S. Zhao, N. Moritz, P. Laurila, R.H. Mattila, L.V.J. Lassila, N. Strandberg, T. Mäntylä, P.K. Vallittu, and H.T. Aro. Development of a biomechanically optimized multicomponent fiber-reinforced composite implant for load-sharing conditions. *Medical Engineering Physics* 31 (2009) 461.
13. S.L. Evans and P.J. Gregson. Composite technology in load-bearing orthopaedic implants. *Biomaterials* 19 (1998) 1329.
14. S. Ramakrishna, J. Mayer, E. Wintermantel, and K.W. Leon. Biomedical applications of polymer-composite materials: A review. *Composites Science and Technology* 61 (2001) 1189.

15. E. Asmussen and A. Peutzfeldt. Influence of UEDMA BisGMA and TEGDMA on selected mechanical properties of experimental resin composites. *Dental Materials* 14 (1998) 51.
16. S.H. Min, J. Ferracane, and I.B. Lee. Effect of shrinkage strain, modulus and instrument compliance on polymerization shrinkage stress of light-cures composites during the initial curing stage. *Dental Materials* 26 (2010) 1024.
17. C. Grimsrud, R. Raven, A.W. Fothergill, and H.T. Kim. The *in vitro* elution characteristics of antifungal-loaded PMMA bone cement and calcium sulphate bone substitute. *Orthopaedics* 34 (2011) 378.
18. M.A. Puska, A.K. Kokkari, T.O. Närhi, and P.K. Vallittu. Mechanical properties of oligomer-modified acrylic bone cement. *Biomaterials* 24 (2003) 417.
19. P.K. Vallittu, I.E. Ruyter, and S. Buykuilmaz. Polymerization time and temperature affects the residual monomer content of denture base polymers. *European Journal of Oral Sciences* 106 (1998) 588.
20. E.K. Viljanen, M. Skrifvars, and P.K. Vallittu. Degree of conversion of an experimental monomer and methyl methacrylate copolymer for dental applications. *Journal of Applied Polymer Science* 93 (2004) 1908.
21. E.K. Viljanen, L.V.J. Lassila, M. Skrifvars, and P.K. Vallittu. Degree of conversion and flexural properties of a dendrimer/methyl methacrylate copolymer: A statistical modeling. *Dental Materials* 21 (2005) 172.
22. S.M.-R. Tuusa, M.A. Puska, L.V.J. Lassila, and P.K. Vallittu. Residual monomers released from glass fiber-reinforced composite photopolymerized in contact with bone and blood. *Journal of Materials Science: Materials in Medicine* 16 (2005) 15.
23. R.L. Bowen. Properties of a silica-reinforced polymer for dental restorations. *Journal of the American Dental Association, JADA* 66 (1963) 57.
24. S. Ruttermann, C. Wandrey, W.H. Raab, and R. Janda. Novel nanoparticles as fillers for an experimental resi-based restorative material. *Acta Biomaterialia* 4 (2008) 1835.
25. S. Garoushi, L.V.J. Lassila, and P.K. Vallittu. Influence of nanometer scale particulate fillers on some properties of microfilled composite resin. *Journal of Materials Science: Materials in Medicine* 22 (2011) 1645.
26. J.T. Heikkilä, A.J. Aho, I. Kangasniemi, and A. Yli-Urpo. Polymethylmethacrylate composites: Disturbed bone formation at the surface of bioactive glass and hydroxyapatite. *Biomaterials* 17 (1996) 1755.
27. P.K. Vallittu. Flexural properties of acrylic polymers reinforced with unidirectional and woven glass fibers. *Journal of Prosthetic Dentistry* 81 (1999) 318.
28. M. Puska, L.V.J. Lassila, P.K. Vallittu, J. Seppälä, and J. Matinlinna. Evaluation of bis-GMA/MMA resin adhesion to silica-coated and silanized titanium. *Adhesion Aspects in Dentistry*. Leiden: VSP (2009) 147.
29. P.K. Vallittu, I.E. Ruyter, and K. Ekstrand. Effect of water storage on the flexural properties of E-glass and silica fiber acrylic resin composite. *International Journal of Prosthodontics* 11 (1998) 340.
30. P.K. Vallittu. Effect of ten years of *in vitro* aging on the flexural properties of fiber-reinforced resin composites. *International Journal of Prosthodontics* 20 (2007) 43.
31. M. Arksornnukit, H. Takahashi, and N. Nishiyama. Effects of silane coupling agent amount on the mechanical properties and hydrolytic durability of composite resin after hot water storage. *Dental Material Journal* 23 (2004) 31.
32. A. Norström, H. Watson, B. Engström, and J. Rosenholm. Treatment of E-glass fibers with acid, base and silanes. *Colloids and Surfaces—Part A: Physicochemical Engineering Aspects* 194 (2001) 143.
33. S. Hansson. The dental implant meets bone—A clash of two paradigms. *Applied Osseointegration Research* 5 (2006) 5.

34. J.M. Bourgery. Traité complet de l'anatomie de l'homme—Part 1: Osteologie. Paris (1832).
35. C. Bell. *Illustration of Paley's Natural Theologie* (1834).
36. J. Wolff. *Das Gesetz der Transformation der Knochen*. Berlin: A. Hirschwald (1892).
37. A. Shinya, A.M. Ballo, L.V.J. Lassila, T.O. Närhi, and P.K. Vallittu. Stress and strain analysis of the bone–implant interface: A comparison of fiber-reinforced composite and titanium implants utilizing 3-dimensional finite element study. *Journal of Oral Implantology* 37 (2011) 133.
38. R.H. Mattila, P. Laurila, J. Rekola, J. Gunn, L.V. Lassila, T. Mäntylä, A.J. Aho, and P.K. Vallittu. Bone attachment to glass fiber-reinforced composite implant with porous surface. *Acta Biomaterialia* 5 (2009) 1639.
39. H. Krenchel. Fiber reinforcement. Thesis. Technical University of Denmark, Copenhagen (1963).
40. A. Tezvergil, L.V.J. Lassila, and P.K. Vallittu. The effect of fiber orientation on the thermal expansion coefficients of the fiber-reinforced composites. *Dental Materials* 19 (2003) 471.
41. E. Anttila, O. Krintilä, T. Laurila, L.V.J. Lassila, P.K. Vallittu, and R. Hernberg. Polymerization shrinkage and hygroscopic expansion of fiber-reinforced composite using fiber Bragg grating sensors. *Dental Materials* 24 (2008) 1720.
42. P.K. Vallittu. Interpenetrating polymer networks (IPNs) in dental polymers and composites. *Journal of Adhesion Science and Technology* 14 (2009) 961.
43. L.V.J. Lassila, J. Tanner, A.M. Le Bell, K. Narva, and P.K. Vallittu. Flexural properties of fiber reinforced root canal posts. *Dental Materials* 20 (2004) 29.
44. L.V.J. Lassila, T. Nohrström, and P.K. Vallittu. The influence of short-term water storage on the flexural properties of unidirectional glass fiber-reinforced composite. *Biomaterials* 23 (2002) 2221.
45. P. Alander, L.V.J. Lassila, and P.K. Vallittu. The span length and cross-sectional design affect values of strength. *Dental Materials* 21 (2005) 347.
46. D.F. Williams. Consensus and definitions in biomaterials. In: *Advances in Biomaterials*, C. de Putter, K. de Lange, K. Groot, and A.J.C. Lee, eds. Amsterdam: Elsevier Science (1988) 11.
47. E. Wintermantel and J. Mayer. Anisotropic biomaterials strategies and developments for bone implants. In: *Encyclopedic Handbook of Biomaterials and Bioengineering—Part B-1*, D.L. Wise, D.J. Trantolo, D.E. Altobelli, J.D. Yaszemiski, J.D. Gresser, and E.R. Schwarzt, eds. New York: Marcel Dekker (1955) 3.
48. P. Christel, L. Claes, and S.A. Brown. Carbon-reinforced composites in orthopaedic surgery. In: *High-Performance Biomaterials: A Comprehensive Guide to Medical and Pharmaceutical Applications*, M. Szycher, ed. Lancaster, PA: Technomic (1991) 499.
49. C. Morrison, R. Macnair, C. MacDonald et al. *In vitro* biocompatibility testing of polymers for orthopaedic implants using cultured fibroblasts and osteoblasts. *Biomaterials* 16 (1995) 987.
50. G. Peluso, L. Ambrosio, M. Cinquegrani, L. Nicolais, S. Saiello, and G. Tajana. Rat peritonela immune response to carbon fiber-reinforced epoxy composite implants. *Biomaterials* 12 (1991) 231.
51. S.M.-R. Tuusa, M.J. Peltola, T. Tirri, L.V.J. Lassila, and P.K. Vallittu. Frontal bone defect repair with experimental glass fiber-reinforced composite with bioactive glass granule coating. *Journal of Biomedical Material Research—Part B: Applied Biomaterials* 82 (2007) 149.
52. S.M.-R. Tuusa, M.J. Peltola, T. Tirri, M.A. Puska, M. Röyttä, H. Aho, J. Saandholm, L.V. Lassila, and P.K. Vallittu. Reconstruction of critical-size calvarial bone defect in rabbits with glass fiber-reinforced composite with bioactive glass granule coating. *Journal of Biomedical Material Research—Part B: Applied Biomaterials* 84 (2008) 510.

53. A.M. Ballo, A. Kokkari, V.V. Meretoja, L.L. Lassila, P.K. Vallittu, and T.O. Närhi. Osteoblast proliferation and maturation on bioactive fiber-reinforced composite. *Journal of Materials Science: Materials in Medicine* 19 (2008) 3169.
54. J.P. Matinlinna, M. Özcan, L.V.J. Lassila, W. Kalk, and P.K. Vallittu. Effect of the cross-linking silane concentration in a novel silane system on bonding resin-composite cement. *Acta Odontologica Scandinavica* 66 (2008) 250.
55. J.P. Matinlinna, J.E. Dahl, S. Karlsson, L.V.J. Lassila, and P.K. Vallittu. The effect of novel silane system to the flexural properties of E-glass fiber-reinforced composites. *Silanes and Other Coupling Agents* 5 (2009) 107.
56. P.K. Vallittu. Comparison of two different silane compounds used for improving adhesion between fibers and acrylic denture base material. *Journal of Oral Rehabilitation* 20 (1993) 241.
57. M. Väkiparta, M.K. Koskinen, P. Vallittu, T. Närhi, and A. Yli-Urpo. *In vitro* cytotoxicity of E-glass fiber weave preimpregnated with novel biopolymer. *Journal of Materials Science: Materials in Medicine* 15 (2004) 69.
58. P.K. Vallittu and K. Ekstrand. *In vitro* cytotoxicity of fiber–polymethyl methacrylate composite used in dentures. *Journal of Oral Rehabilitation* 26 (1999) 666.
59. M. Hautamäki, V.V. Meretoja, R.H. Mattila, A.J. Aho, and P.K. Vallittu. Osteoblast response to polymethyl methacrylate bioactive glass composite. *Journal of Materials Science: Materials in Medicine* 21 (2010) 1685.
60. A.M. Ballo, E.A. Akca, T. Ozen, L. Lassila, P.K. Vallittu, and T.O. Närhi. Bone tissue responses to glass fiber-reinforced composite implants—A histometric study. *Clinical Oral Implants Research* 20 (2009) 608.
61. R.M. Day. Bioactive glass stimulates the secretion of angiogenetic growth factors and angiogenesis *in vitro*. *Tissue Engineering* 11 (2005) 768.
62. P. Stoor, E. Söderling, and R. Grenman. Interactions between the bioactive glass S53P4 and the atrophic rhinitis–associated microorganism *Klebsiella ozaenae. Journal of Biomedical Materials Research—Part B: Applied Biomaterials* 48 (1999) 869.
63. L.L. Hench and J. Wilson. Surface active biomaterials. *Science* 226 (1984) 630.
64. L.L. Hench and H.A. Paschal. Direct chemical bond of bioactive glass–ceramic materials to bone and muscle. *Journal of Biomedical Materials Research* 4 (1973) 25.
65. Ö.H. Andersson and I. Kangasniemi. Calcium phosphate formation at the surface of bioactive glass *in vitro*. *Journal of Biomedical Materials Research* 24 (1991) 1019.
66. Ö.H. Andersson, K.H. Karlsson, and K. Kangasniemi. Calcium phosphate formation at the surface of bioactive glass *in vivo*. *Journal of Noncrystalline Solids* 119 (1990) 290.
67. N.C. Lindfors, P. Hyvönen, M. Nyyssönen et al. Bioactive glass S53P4 as bone graft substitute in treatment of osteomyelitis. *Bone* 47 (2010) 212.
68. A.J. Aho, E. Suominen, A. Alanen, A. Yli-Urpo, J. Knuuti, and H.J. Aho. Remodelling of the tibia after grafting of a large cavity with particulate bioactive glass–hydroxyapatite—Case report on treatment of fibrous dysplasia with 13 years' follow-up. *Acta Orthopaedica Scandinavica* 74 (2003) 766.
69. D.S. Zhao, N. Moritz, P. Laurila, R. Mattila, L.V. Lassila, N. Strandberg, T. Mäntylä, and H. Aro. Development of a multicomponent fiber-reinforced composite implant for load-sharing conditions. *Medical Engineering and Physics* 31 (2009) 461.
70. A.M. Ballo, E.A. Akca, T. Ozen, L.V. Lassila, P.K. Vallittu, and T.O. Närhi. Bone tissue responses to glass fiber-reinforced composite implants—A histometric study. *Clinical Oral Implants Research* 6 (2009) 608.
71. A.M. Ballo, T.O. Närhi, E.A. Akca, T. Ozed, S.M. Syrjänen, L.V. Lkassila, and P.K. Vallittu. Prepolymerized versus *in situ* polymerized fiber-reinforced composite implants—A pilot study. *Journal of Dental Research* 90 (2011) 263.

72. A. Mareira-Gonzalez, I.T. Jackson, T.T. Miyawaki, K. Barakat, and V. DiNick. Clinical outcome in cranioplasty: Critical review in long-term follow-up. *Journal of Craniofacial Surgery* 14 (2003) 114.
73. N. Sahoo, I.D. Roy, A.P. Desai, and V. Gupta. Comparative evaluation of autogenous calvarial bone graft and alloplastic materials for secondary reconstruction of cranial defects. *Journal of Craniofacial Surgery* 21 (2010) 79.
74. E.J. Stelnicki and D.K. Ousterhout. Prevention of thermal injury induced by application of polymethylmethacrylate to the calvarioum. *Journal of Craniofacial Surgery* 7 (1996) 192.
75. P.K. Vallittu. Peak temperature of some prosthetic acrylates on polymerization. *Journal of Oral Rehabilitation* 23 (1996) 776.
76. M.J. Peltola, P.K. Vallittu, V. Vuorinen, A.A. Aho, A. Puntala, and K.M. Aitasalo. 2011. Novel composite implant in craniofacial bone reconstruction. *European Archives of Otorhinolaryngology* 269 (2012) 623.
77. K. Aitasalo, M. Peltola, V. Vuorinen, and P. Vallittu. *Novel Composite Implants in Craniofacial Reconstruction*. North American Skull Base Society, Los Angeles, CA (2009).

2 Bioceramic and Biopolymer Nanocomposite Materials for Use in Orthopedic Applications

Clark E. Barrett, Ruth E. Cameron, and Serena M. Best

CONTENTS

2.1 INTRODUCTION

Bone is an organ capable of self-repair following an injury. However, the loss of significant bone volume due to infection or trauma may result in a permanent defect at an injury site. Current surgical techniques employed to repair large defects include bone grafting and metallic implants. Bone grafting is limited by the quantity of bone available from a possible donor site, making the procedure unsuitable for large defects. Metallic implants are of particular use in load-bearing environments due to their high strength and toughness. However, these devices are far from optimal

solutions due to stress shielding (Park and Lakes 1992) and associated bone atrophy, which is often a cause of device loosening and ultimate failure (Wolff 1987). Long-term metallic implant concerns involve potential cytotoxicity arising from heavy metal ion liberation and harmful corrosion products (Williams 1981).

Much research has been undertaken with the aim of optimizing osseointegration on metal surfaces that possess nanometer-scale topographic features. Often, these techniques incorporate hydroxyapatite (HA) and various substituted HA types (Best et al. 2008). Nanomanipulation is not limited to the bone—surface nanopatterning is employed in the cartilage, vascular tissue, bladder, and other tissue engineering applications.

A basic literature search reveals a plethora of investigations into polymer–ceramic nanocomposite (PMNC) development for clinical use which is logical considering the number of degrees of freedom in these systems. PMNCs are defined as polymers containing a ceramic phase that possesses at least one dimension less than 100 nm. Due to the manifold variables that determine PMNC behavior, this chapter considers only a limited number of materials used in PMNC designs. Emphasis is given to the effects of nanoceramic addition on material properties: degradation kinetics, mechanical and biological effects (Sections 2.3.1, 2.3.2, and 2.3.4), and the specific changes manifest by nanoparticles as opposed to conventional microparticle inclusions. Furthermore, modeling attempts to account for modifications to material parameters effected by nanoparticle properties are reported (Section 2.4).

In order to account for nanoparticle effects in these materials, it is first necessary to describe other material properties and modifications wrought by nanoscale phenomena. To this end, some of the most common polymers and ceramics used in osseous tissue regeneration are elucidated in Sections 2.2.1 and 2.2.2 before proceeding to nanoparticle effects on material properties.

2.2 MATERIALS

2.2.1 Polymers

The use of polymers in prostheses is long established and widespread. The choice of polymer that may be used in a biological implant is limited by the requirements that the polymer be nontoxic, biocompatible, and biodegradable and the material's degradation products should have no negative effects on the surrounding tissues and organs of a host organism (Yang et al. 2006). Most available polymeric devices currently on the market do not degrade *in vivo*, e.g., ultra high molecular weight polyethylene, which is used in total hip replacements (Wang 2004). The majority of polymers investigated for osseous tissue regeneration or defect filling pertain to the polyester family to which poly(α-hydroxy acids) [incorporating polylactide (PLA), polyglycolide, and their copolymers] belong (Balasundaram and Webster 2007). A biopolymer's mechanical properties, biological effects, and degradation kinetics are influenced by its hydrophobicity, molecular weight distribution, glass transition temperature, crystallinity, geometry, temperature, and polymer processing technique. Accordingly, a wide range of possibilities exist to manipulate a polymer's properties to suit different requirements. In addition, radiation is often used as a sterilization

method prior to clinical use; therefore, the effects of radiation damage have been investigated to ascertain changes to molecular weight, glass transition temperatures, and other properties with demonstrable effects (Yoshioka et al. 1995; Tan et al. 2009).

Poly(α-hydroxy acids) have a long history of the U.S. Food and Drug Administration (FDA)-approved use in medical devices and a large variation in properties between different poly(lactic-co-glycolic acid) (PLGA) forms, making this class of polymer a preferred candidate for a resorbable tissue engineering scaffold polymeric phase (Li et al. 1990; Lu et al. 2000). PLGA and other polyesters degrade by hydrolysis (or partly via enzymatic action *in vivo*), producing lactic acid, which is metabolized by the body via the tricarboxylic acid cycle to be excreted as CO_2 and H_2O (Holland et al. 1986), and glycolic acid, which is excreted in urine.

Polyester degradation in an aqueous environment is classified as bulk heterogeneous degradation in which de-esterification is catalyzed by $H^+_{(aq)}$ ions generated by acid dissociation of degradation products. The acids also diffuse through the material; hence, degradation is a reaction–diffusion problem, depending on material geometry, oligomer diffusion coefficients, and associated boundary conditions, among other factors. Due to autocatalysis, acid accumulates at the center of the material, whereas acids produced closer to the material boundary may diffuse into the surrounding medium, resulting in position- and time-dependent degradation rates with de-esterification proceeding faster at the material center compared to the boundary. Accumulation of acidic degradation products from PLGA has been shown to induce chronic inflammatory responses *in vivo* and a propensity to elicit fibrous tissue encapsulation at the polymer–hose interface (Lickorish et al. 2007); fibrosis at the implant–bone interface can cause device failure at early degradation times (Athanasiou et al. 1996). For more information regarding PLGA degradation, the reader is directed to the work of Therin et al. (1992) and Li et al. (1990).

In this chapter, the D,L-lactide/glycolide molar ratio in PLGA studies is given in parentheses. A plethora of other biodegradable polymers have been extensively investigated, and a brief description of some common types is given in Table 2.1.

The motivations for ceramic nanoparticle addition to polymers include possible improvements to degradation kinetics control offered by polymer–ceramic microcomposites, biological enhancement, and possible nanoparticle stiffening improvements to PMNC mechanical properties affected by nanoparticle addition. PMNCs

TABLE 2.1
Material Properties of Various Biopolymers

Polymer	Crystallinity	Tensile Strength (MPa)	Young's Modulus (GPa)	Approximate Degradation Time
Polyglycolide	Semicrystalline	~70	~6	6–12 months
Polycaprolactone	Semicrystalline	20–25	0.4	~3 years
Poly-L-lactide	Semicrystalline	60–70	3	~3 years
Collagen	Variable	50–100	1	–

are viewed as an evolution of traditional micrometer-sized polymer–ceramic composites. Basic properties of the most commonly used ceramics are described in Sections 2.2.2 and 2.2.2.1.

2.2.2 Ceramics

The concept of the incorporation of HA or another bioceramic to a polymer was introduced by Bonfield et al. (1981) based on the observation that the bone consists of an organic matrix reinforced with a mineral phase. Nanocrystalline HA is similar in composition to the main inorganic constituent of the bone. Consequently, many scaffold designs are based on or have incorporated HA as the primary ceramic phase. Nevertheless, the physical properties and mechanical reliability of pure HA ceramics are poor compared to the bone and, for this reason, is principally used in the form of powders, implant coatings, low-loaded porous implants, and bone cement (Best et al. 2008; Lewandrowski et al. 2000). HA exhibits low biodegradability, with some studies reporting incomplete reabsorption of sintered HA after 9 months *in vivo* (Klein et al. 1983). Numerous investigations have attested to enhanced osteoconductivity and osteoblast metabolism on nanoscale HA (Huang et al. 2004; Pezzatini et al. 2006). Much research has focused on modifying the chemical properties of HA to enhance its osteoconductivity; the interested reader is directed to the summary in the work of Suchanek et al. (1997).

For certain applications, high ceramic degradation rates are required; hence, interest in the tricalcium phosphate (TCP) $Ca_3(PO_4)_2$ class of bioceramic has increased. TCP has four known polymorphs: α, β, γ, and super-alpha ($\overline{\alpha}$). The $\overline{\alpha}$ and γ phases are only observed at high temperatures and pressures (Nurse et al. 1959). The β phase is the most stable form at standard temperature and pressure; the α phase is thermodynamically stable between 1120°C and 1470°C in the absence of impurities (Dorozhkin 2009) and occurs at room temperature by quenching or rapid cooling from its stable state. Both α- and β-TCPs are prepared by the thermal decomposition of calcium-deficient HA, and often, both TCP phases occur with HA after processing (Gibson et al. 1996).

2.2.2.1 Calcium Phosphate Solubility and pH Buffering Reactions

The acidity solubility regimes and apatite reactions with carboxylic acids are fundamental phenomena in composite behavior and affect local pH variant autocatalysis (see Sections 2.2.1 and 2.4). There are only three stable calcium phosphates at standard temperature and pressure: (1) monocalcium phosphate monohydrate [$Ca(H_2PO_4)_2$, pH < 2.51]; (2) brushite ($CaHPO_4 \cdot 2H_2O$, 1.5 < pH < 4.2); and (3) HA (pH > 4.2; Driessens 1982). The pH dependence on solubility is an important factor of any model of these materials' temporal and spatial degradation. The solubility of α- and β-TCP at pH 7.4 is $K_{sp}^{\alpha} = 10^{-25.5}$ and $K_{sp}^{\beta} = 10^{-29.5}$, respectively (Bohner et al. 1997). HA possesses a much lower solubility product at pH 7.4 ($K_{sp}^{HA} = 10^{58.6}$) (Fernández et al. 1999). Dissolved TCP, given a sufficient concentration of calcium and phosphate ions, will reprecipitate as HA, which is the only stable calcium phosphate at standard temperature and pressure, forming an HA bounding layer on TCP crystal surfaces (Klein et al. 1990; cf., Figure 2.1).

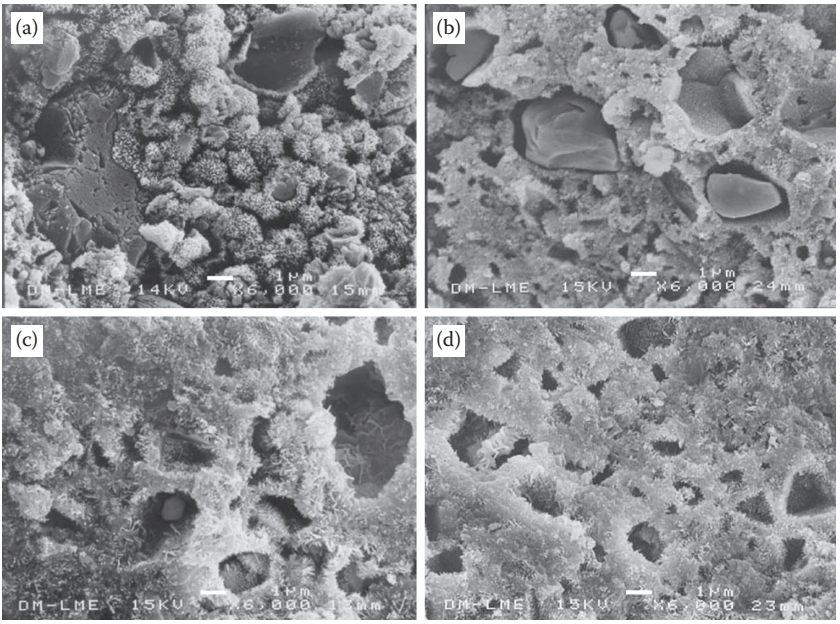

FIGURE 2.1 Evolution of the structure of α-TCP crystals observed using scanning electron microscopy (SEM) after (a) 2 h, (b) 8 h, (c) 64 h, (d) and 360 h in aqueous medium. (From Ginebra, M.P. et al., Effect of the particle size on the micro and nanostructural features of a calcium phosphate cement: A kinetic analysis, *Biomaterials*, 25, 3453, 2003. Reproduced with permission from Elsevier.)

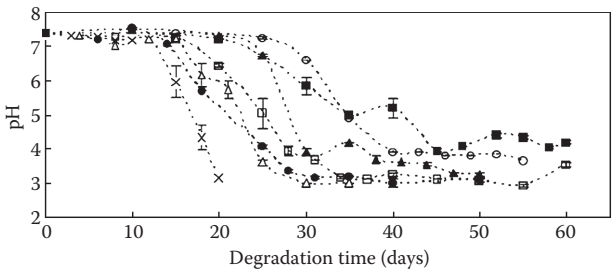

FIGURE 2.2 Variation of pH of solution containing α-TCP–PLGA composite materials as a function of degradation time. ×, Pure PLGA; Δ, 5% TCP; ●, 10% TCP; □, 15% TCP; ▲, 20% TCP; ○, 30% TCP; ■, 40% TCP. (From Ehrenfried, L.M. et al., Mechanical behavior of interpenetrating co-continuous beta-TCP–PDLLA composites, *Bioceramics*, 20, 361, 2008. Reproduced with permission from Elsevier.)

A primary reason for the ceramic addition to PMNCs is to buffer acidity and to modify degradation kinetics in the degrading nanocomposite (see Figure 2.2). The end scission reaction of PLGA autocatalyzed by H^+_{aq} may be written as

$$\text{PLGA} + H_2O \xrightarrow{H^+} R - COOH + R - OH. \tag{2.1}$$

The carboxylic acid has a high degree of acid dissociation, and thus, degradation releases H^+_{aq}, which autocatalyzes further hydrolysis, i.e.,

$$R - COOH \quad R - COO + H^+_{aq}. \tag{2.2}$$

In an aqueous medium, the calcium phosphate dissociates to form

$$Ca_3(PO_4)_2 \quad Ca^{2+}_{aq} + (PO^{3-}_4)_{aq}. \tag{2.3}$$

The phosphate ions subsequently react with the hydrons via the buffering reactions, forming monohydrogen phosphate

$$PO^{3-}_4 + H^+ \quad HPO^{2-}_4 \tag{2.4}$$

dihydrogen phosphate

$$PO^{3-}_4 + H^+ \quad H_2PO^-_4 \tag{2.5}$$

and phosphoric acid

$$H_2PO^-_4 + H^+ \quad H_3PO_4. \tag{2.6}$$

Equations 2.4 through 2.6 elucidate the mechanisms that remove catalytic H^+_{aq} from the solution. TCP and HA dissolution is affected by acidity, physical disintegration into small particles due to preferential dissolution at grain boundaries, and biological factors (Lu et al. 2002). Equations 2.2 through 2.6 are important in nanocomposite material modeling incorporating a ceramic phase (Section 2.4).

2.2.3 Other Constituents

Further considerations to PMNC design include improved coupling between the mineral and organic phases. Numerous investigations have highlighted the critical role played by polymer–ceramic bonding interactions in reducing nanoparticle agglomeration (Jancar and Kucera 1990) or improving mechanical properties (either by reductions in stress concentrations in the polymer matrix or indirectly via T_g manipulation), especially when considering device degradation and performance in an aqueous environment. The interaction strength between the two phases has important ramifications for material behavior, specifically mechanical behavior and glass transition temperature modifications, which are further addressed in Sections 2.3.2 and 2.3.3. Often, only physical adsorption is achieved between the polymeric and ceramic phases. To address this, the ceramic surface may be treated to become more chemically compatible with the polymer matrix (Hong et al. 2005). A common reactive treatment is the incorporation of silanes to the surface of the ceramic phase, which results in increased end-group availability fomenting stronger polymer–ceramic bonding (Jancar and Kucera 1990). Thus, the interaction between the inorganic

surface and the matrix polymer can be tuned by selecting appropriate end groups. These considerations, albeit important with regard to nanocomposite behavior, are not considered in detail in this chapter. For a treatise on the silane treatment of fillers, the reader is directed to the work of Plueddemann (1991).

Other PMNC topics that will not be discussed include the addition of growth factors such as bone morphogenic proteins (Wozney 2002) to induce new bone formation and a plethora of other factors, including scaffold geometry, that play important roles in degradation kinetics (Braunecker et al. 2004).

2.3 MATERIAL PROPERTIES

2.3.1 Nanocomposite Degradation Behavior and Acidity Regulation

TCP–PLGA composite acidity buffering capacity generally improves with TCP content (Ehrenfried et al. 2008; Wang 2004). Yang et al. (2009) degraded α-TCP–PLGA(50:50) composites with varying weight ceramic loadings and particle sizes in simulated body fluid (SBF). Differences in degradation kinetics are shown in Figures 2.3 and 2.4. Figure 2.3 clearly demonstrates the reduction in composite degradation rates due to reaction rate modification resulting from the ceramic inhibition of the autocatalytic effect. Moreover, Figure 2.3 shows ceramic crystal-size effects, with 30 wt% nanocomposites exhibiting a delay of approximately 7 days in pH change, onset of polymer mass loss, and time of maximum water absorption compared to

FIGURE 2.3 Morphological state of α-TCP–PLGA(50:50) nanocomposites at different degradation times in phosphate-buffered saline (PBS). (a) and (b) α-TCP (30 wt%) and nanocomposite (20 wt%) after 43 days. (c) Pure PLGA(50:50) at 21 days. (d) Microcomposite (30 wt%) at 36 days. (From Yang, Z. et al., The influence of α-tricalcium phosphate nanoparticles and microparticles on the degradation of poly(D,L-lactide-coglycolide), *Advanced Materials*, 21, 3900, 2009. Reproduced with permission from Wiley.)

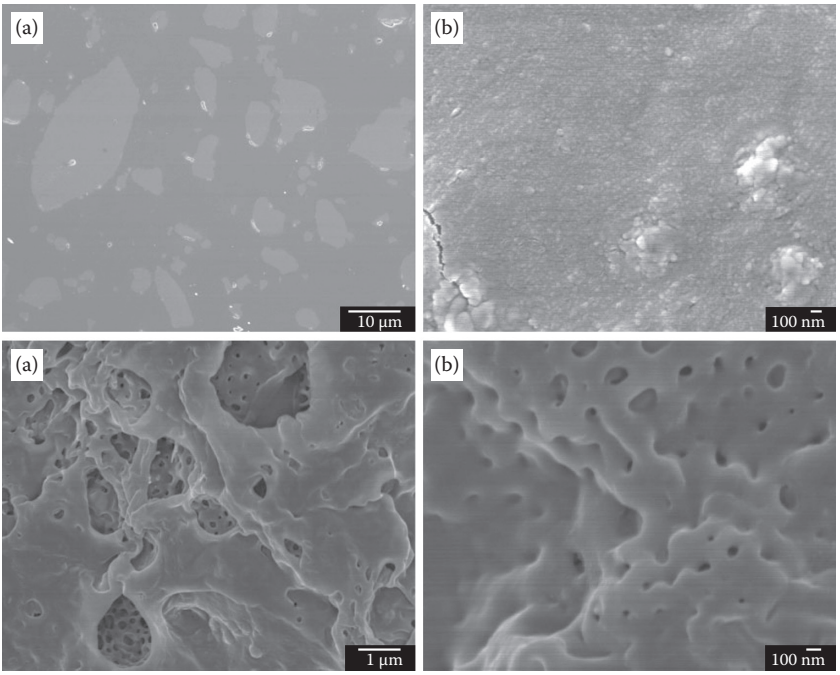

FIGURE 2.4 SEM images of 30 wt% α-TCP–PLGA(50:50) microcomposites and nanocomposites at various degradation times *in vitro* in SBF. (a) Undegraded microcomposite. (b) Microcomposite degraded for 36 days. (c) Undegraded nanocomposite. (d) Nanocomposite degraded for 30 days. (From Yang, Z. et al., The influence of α-tricalcium phosphate nanoparticles and microparticles on the degradation of poly(D,L-lactide-coglycolide), *Advanced Materials*, 21, 3900, 2009. Reproduced with permission from Wiley.)

the equivalent microcomposite. A comparison of surface morphologies for both composite types at different times is shown in Figure 2.4.

The overall pH change in buffering medium during *in vitro* degradation is independent of ceramic particle size, although the rate of pH change is observed to be particle size dependent, with nanoparticles exhibiting a slower pH decrease during degradation. This is important, as slower changes allow acids to be removed by the body, preventing accumulation and cytotoxicity. However, numerous studies have established that, above particular ceramic weight loadings (approximately 30%), little change in degradation kinetics or acid release profile is observed. This convergence has often been attributed to nanoparticle agglomeration, which is now challenged by new material modeling results, as summarized in Section 2.4.

Tang et al. (2008) investigated the water absorption of poly(3-hydroxybutyrate-co-3-hydroxyvalerate)/HA nanocomposites using a standard Fickian diffusion description (Becker et al. 2004; Chuang et al. 2004). The nano-HA used in the study was modified with a silane coupling agent. Water absorption in the materials is greatly affected by HA leaching. Furthermore, water diffusion coefficients have an inverse

relationship with nano-HA filler content, although diffusion coefficients remained within the same order of magnitude for all composite types.

2.3.2 Mechanical Behavior

There is much evidence regarding the enhancement of biopolymer mechanical strength by the incorporation of nanoparticulate bioceramics. McManus et al. (2005) reported significantly greater bending moduli in PLA containing 40 and 50 wt% nanophase alumina, titania, and HA than composites with coarser grained ceramics. Liu and Webster (2010) characterized the compressive and tensile properties of composites composed of dispersed and agglomerated particles of 30 wt% HA and titania contained in PLGA(50:50) matrices. Titania nanocomposites exhibited superior elastic and bulk moduli and greater tensile strength at yield than pure PLGA and agglomerated composites, whereas dispersed nano-HA demonstrated inferior moduli but greater ductility than the agglomerated composite. Nano titania and HA composite differences were attributed to different polymer–ceramic bonding strengths.

PMNC nanoparticle effects may be expressed directly as a matrix stiffener or indirectly by changing the polymer phase's thermodynamic state by modifying the material's glass transition temperature, T_g. Wilberforce et al. (2001, 2010) reported large T_g reductions with increasing nano α-TCP loadings in PLGA(50:50), which were attributed to the large interfacial area and poor polymer–ceramic bonding. Results from expanding the study to gauge changes wrought by differing polymer-processing methods are presented in Figure 2.5, which demonstrates T_g reduction due to polymer–ceramic interface effects (variations between polymer-processing routes probably result from polymer thermal degradation during solvent evaporation). Also shown in Figure 2.5 is the dramatic effect of water diffusion and material plasticization, which is detrimental to the composite's mechanical strength—an important factor influencing composite behavior, which is further assessed in Section 2.3.3.

The transition to a rubbery state in polymers results in increased polymer chain mobility and significant changes to material properties. Elastic polymers are much more viscoelastic and present reduced storage moduli for $T > T_g$ than in the glassy state. Consequently, systematic studies and empirical descriptions of MPNC T_g variation with the ceramic interface area, polymer–ceramic bonding, water content and other factors affecting T_g are required.

Neglecting material property changes at temperatures close to T_g, numerous studies have demonstrated that, in general, a polymer's bulk and elastic moduli increase with the incorporation of nanoparticles with the increase being proportional to the nanoparticle loading and increasing for smaller particles. The strengthening mechanism is not understood completely (Hu et al. 2010). Mechanical deformation theory indicates that the high-volume fraction of interfacial regions compared to bulk materials leads to increased deformation by grain-boundary sliding and short-range diffusion-healing events as the grain size is reduced, thus increasing ductility for nanocrystalline ceramics (Narayan et al. 2004). This issue is complicated close to T_g and is exemplified in Figure 2.6, which shows the storage modulus of α-TCP–PLGA(50:50) nanocomposites prepared by injection molding as a function

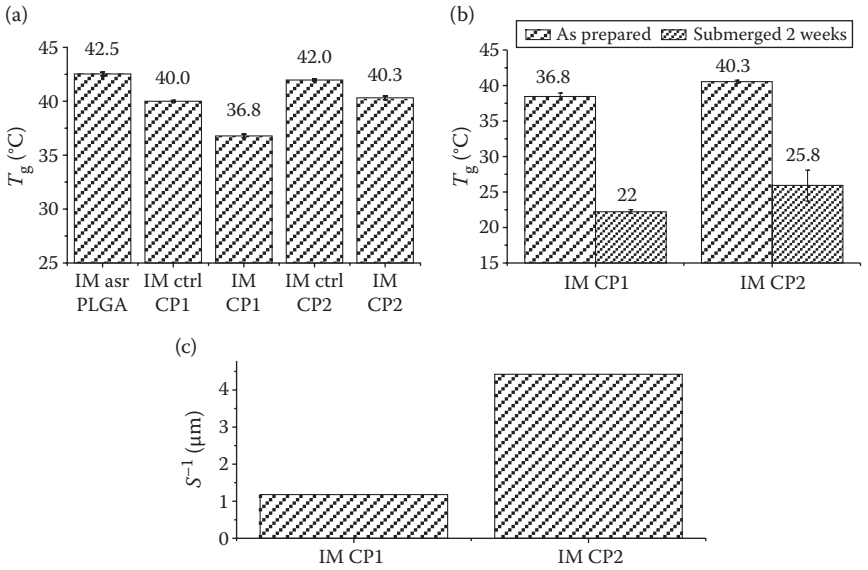

FIGURE 2.5 (a) T_g measured using differential scanning calorimetry of injection-molded samples (IM) processed via solvent evaporation (CP1) or twin screw extrusion (CP2). IM asr PLGA denotes injection-molded PLGA as received from the supplier. IM Ctrl CP1 and IM Ctrl CP2 represent injection-molded PLGA prepared and compacted via solvent evaporation and twin screw extrusion, respectively, which are used as controls. (b) T_g of samples after 2 weeks of degradation in PBS solution. (c) Reciprocal surface area of α-TCP particles per unit volume of composite. (From Wilberforce, S.I.J. et al., The influence of the compounding process and testing conditions on the compressive mechanical properties of poly(D,L-lactide-co-glycolide)/α-tricalcium phosphate nanocomposites, *Journal of Biomedical Materials Research*, 4, 1081, 2001. Reproduced with kind permission from Springer.)

of temperature (Wilberforce et al. 2010). The pure polymer exhibits the largest T_g, which is approximately 50°C, and the lowest T_g occurs in the 30 wt% nanocomposite. The higher ceramic loaded PMNCs demonstrate higher transition temperatures due to particle agglomeration in these samples, which indicates that the phenomenon is attributable to nanoparticle effects. Far from T_g, the storage modulus increases with filler content. However, due to nanoparticle-induced changes in T_g and subsequent deterioration of mechanical strength, at body temperature, any enhancement of PLGA(50:50) properties caused by nanoparticle addition is lost, and the pure polymer possesses superior properties. Consequently, nanoparticle addition to some polymers such as PLGA and resulting T_g reduction might be detrimental to the desired materials' mechanical properties compared to pure polymer or conventional microcomposites. This factor is considered further in Section 2.3.3. Wilberforce et al. (2011) showed that the addition of α-TCP nanoparticles to poly-L-lactide (PLLA), followed by quenching or annealing, reduced the T_g to a minimum of 60°C, making

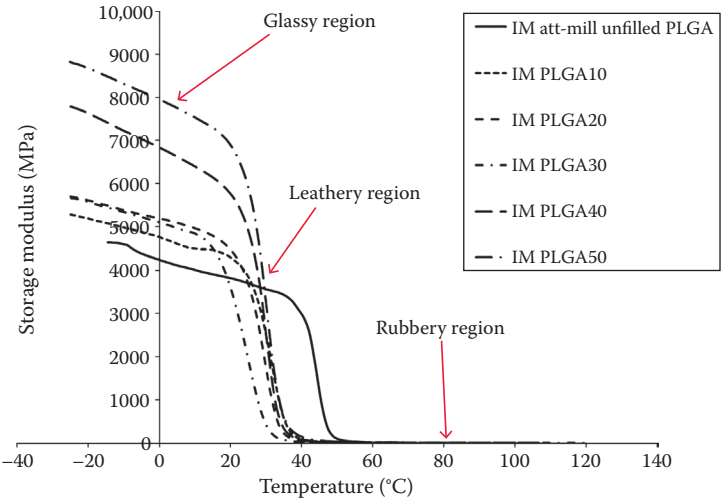

FIGURE 2.6 Storage modulus as a function of temperature measured by dynamical mechanical testing performed at 1 Hz for dry nano α-TCP–PLGA(50:50), with different ceramic weight loadings illustrating the critical role of T_g on mechanical properties of PLGA PMNCs. (From Wilberforce, S.I.J. et al., A dynamic mechanical thermal analysis study of the viscoelastic properties and glass transition temperature behavior of bioresorbable polymer matrix nanocomposites, *Journal of Materials Science: Materials in Medicine*, 21, 3085, 2010. Reproduced with kind permission from Springer.)

rubber transition effects unimportant at body temperature (pure PLLA exhibits a glass transition at approximately 70°C).

2.3.3 Glass Transition Behavior

Reductions in T_g as a function of film thickness have been well documented for polymer nanofilms (Ash et al. 2002). Bulk polymers may be described as having two regions with two different glass transition temperatures for the surface and bulk, T_g^{surf} and T_g^{bulk}, respectively. The surface layer extends to approximately 100 nm from the surface and is hypothesized to represent a liquid-like surface layer with increased polymer mobility compared to a bulk polymer substratum (Keddie et al. 1994). For a freestanding pure polymer thin film of total thickness h, the contribution of the surface and bulk glass transition temperatures to the total material glass transition temperature as a function of film thickness is

$$T_g(h) = T_g^{bulk} + \frac{2\varepsilon}{h}\left(T_g^{surf} - T_g^{bulk}\right) \tag{2.7}$$

where ε represents the surface region thickness. This description assumes a freestanding polymer film that produces the largest change in T_g. Glass transition temperature

deviations are observed in supported films whereby the change in T_g depends on the strength of the interaction between the polymer and the substrate. Polymer–substrate interfaces exhibiting attractive interface properties (wetting) and those with weak interactions (nonwetting) manifest T_g increases and decreases, respectively (Ellison et al. 2005). Interfacial polymer–ceramic properties play a critical role in composite mechanical properties (Charvet et al. 2000). Moreover, improvements in polymer–ceramic wettability aid nanoparticle dispersion, as demonstrated by Guo et al. (2008), in which improved nanoparticle dispersion and consequent tensile strength increases were observed for Fe_2O_3 nanoparticle–resin composite treated using the bifunctional coupling agent methacryloxypropyltrimethoxysilane compared to uncoupled nanocomposites.

Bansal et al. (2005) demonstrated an equivalence principle between thermomechanical thin film properties and polymer–nanoparticle surface interactions in PMNCs. The authors calculated three-dimensional average particle separations of silica nanoparticles dispersed in polystyrene (PS) from transmission electron microscopy images and showed a good correlation between T_g as a function of particle separation for the composites and T_g as a function of polymer film thickness for PS–silica nanocomposites (cf., Figure 2.7).

PMNCs exhibit a wide variation in glass transition temperature, which depends on factors such as polymer and nanoparticle composition, solvent extraction, and nanoparticle sizes and loadings (Section 2.3.2). Generally, increasing the polymer's molecular order and greater intermolecular energy raises T_g (Donth 2001). As a general rule, T_g increases for larger polymer cohesive energies and greater molecular order, i.e.,

$$T_g = \frac{\Delta H}{\Delta S} \tag{2.8}$$

where ΔH and ΔS represent the enthalpy and entropy changes wrought by the transition to a rubbery state, respectively. Increasing polymer cross-linking results in greater cohesion energy, which raises ΔH. More importantly, in view of water-induced plasticization (cf., Figure 2.5), composite water absorption increases the system disorder, which can result in a dramatic T_g decrease.

The structural relaxation (aging) of polymers is a closely related phenomenon to T_g surface modification, which is influenced by interface effects with relaxation rate changes caused by surface interactions extending more than 100 nm into the film interior (Priestley et al. 2005). The authors believe these phenomena to be of great importance in designing PMNCs for clinical use, not only in the assessment of device behavior in the laboratory but also in aging-induced changes in properties due to storage time before device implantation in patients. Moreover, these properties must be addressed for all PMNC types and also evaluated as a function of degradation time. Furthermore, nanoparticle-induced changes in composite mechanical properties and aging can be modified by the use of binding agents, which warrants further development.

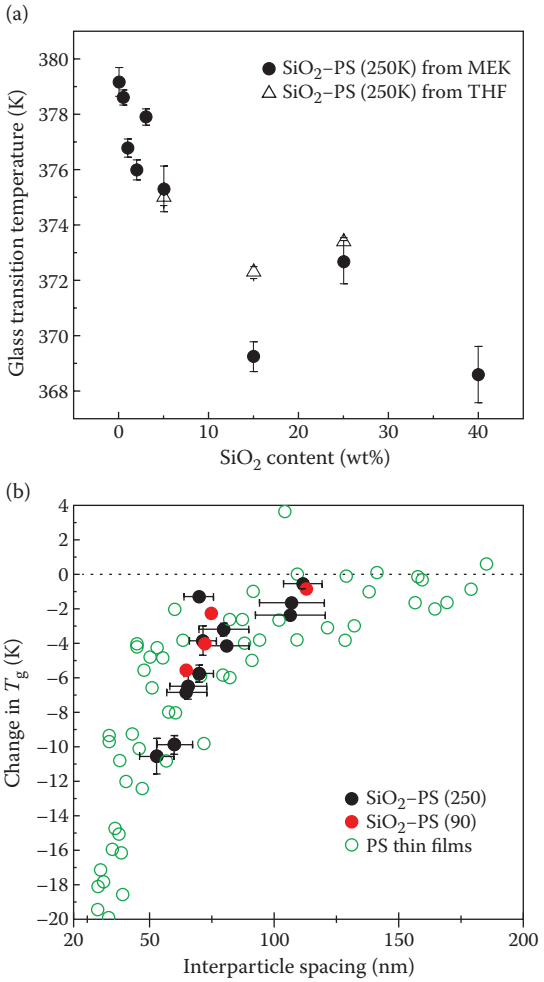

FIGURE 2.7 (a) T_g of SiO_2–PS nanocomposites as a function of silica weight content for composites prepared using the solvents methyl ethyl ketone (MEK) and tetrahydrofuran (THF). Large deviations observed at high weight loadings are caused by particle agglomeration. (b) Comparison between T_g reduction measured for thin PS films as a function of film thickness and T_g reduction of PS–silica nanocomposites as a function of mean interparticle spacing. Numbers in parentheses denote matrix molecular weight. (From Bansal, A. et al., Quantitative equivalence between polymer nanocomposites and thin polymer films, *Nature*, 4, 693, 2005. Courtesy of Nature Publishing Group.)

2.3.4 Bioactivity

Yang et al. (2008) evaluated the *in vitro* bioactivity of nanostructured α-TCP–PLGA(75:25) composites by quantifying the rapid formation of bonelike apatite layers on the material's surface while immersed in SBF (the α phase was chosen due to its greater solubility than β-TCP). Enhanced apatite nucleation and dense

lamellar-like apatite formation were observed after 7 and 14 days of immersion, respectively. Acellular indicators of improved bioactivity were corroborated by *in vitro* cell culture studies using human osteoblast-like (HOB) cells, elucidating greater cell numbers on the nanocomposite as the culture proceeded and the observation of a confluent lamellar-like apatite layer beneath a proliferating HOB layer at day 16. Enhanced apatite nucleation was attributed to the nanostructured surface providing large numbers of nucleation sites for apatite precipitation or fast dissolution of nanoparticles near the surface. Both of these mechanisms most likely work in conjunction to create rougher surface topographies. In addition, in a later study, Yang et al. (2009) reported the liberation of residual micron-scale ceramic particles (which are known to cause adverse cell response) from the microcomposite into the buffer medium, which did not occur in the nanocomposites.

Biocompatibility enhancement is not confined to calcium phosphate addition; other nanoceramics such as titania and alumina have demonstrated the inducement of improved cell function (Webster et al. 1999, 2000a). Nanophase titania–PLGA(50:50) composites investigated by Liu et al. (2006) demonstrated that the greatest *in vitro* osteoblast adhesion and optimal indicators of bioactivity such as collagen, alkaline phosphatase activity, intracellular and extracellular protein synthesis, and calcium-containing mineral deposition occurred for composites possessing surface roughness values, which most closely matched that of the natural bone (cf., Figure 2.8). In addition, the material surface roughness as opposed to ceramic surface coverage was shown to dominate the cell response. The surface topographic effect is not limited to bioceramics. Webster and Ejiofor (2004) analyzed osteoblast adhesion on several nanophase metals, which exhibited increased osteoblast adhesion to nanopatterned surfaces relative to conventional surfaces presenting micrometer-sized topographic features. Interestingly, the study observed preferential osteoblast adhesion at grain boundaries.

The compendium of studies performed to assay cell responses to nanometer-sized topographic surface modification clearly demonstrates that nanometer topographies alter cell behavior significantly. In the study of Palin et al. (2005), the authors sought to assess the preponderance of nanoscale topography over extraneous factors such as surface chemistry and surface energy. To this end, nanometer-scale and conventional topographic structures were formed on PLGA by molding and seeded with osteoblasts. The bioactivities of the different surfaces were assessed by quantifying osteoblast proliferation as a function of time, with nanopatterned PLGA demonstrating more than double the initial number of adhered osteoblasts than the conventional surface after 1 day and 5 days in culture.

Enhancing osteoclast activity is also important for nanocomposite clinical performance; rapid bone deposition mediated by osteoblasts and remodeling via osteoclasts is a vital component of wound healing and the incorporation of the orthopedic device. Webster et al. (2001) showed that indicators of osteoclast activity, the number of resorption pits, and tartrate-resistant acid phosphatase increased on nanophase alumina and HA compared to conventional-sized particles. Increased wettability or hydrophilicity is associated with increased protein absorption and, consequently, increased cell adhesion and enhanced function. The study showed increased numbers of absorption pits on nanometer surfaces compared to micro surfaces.

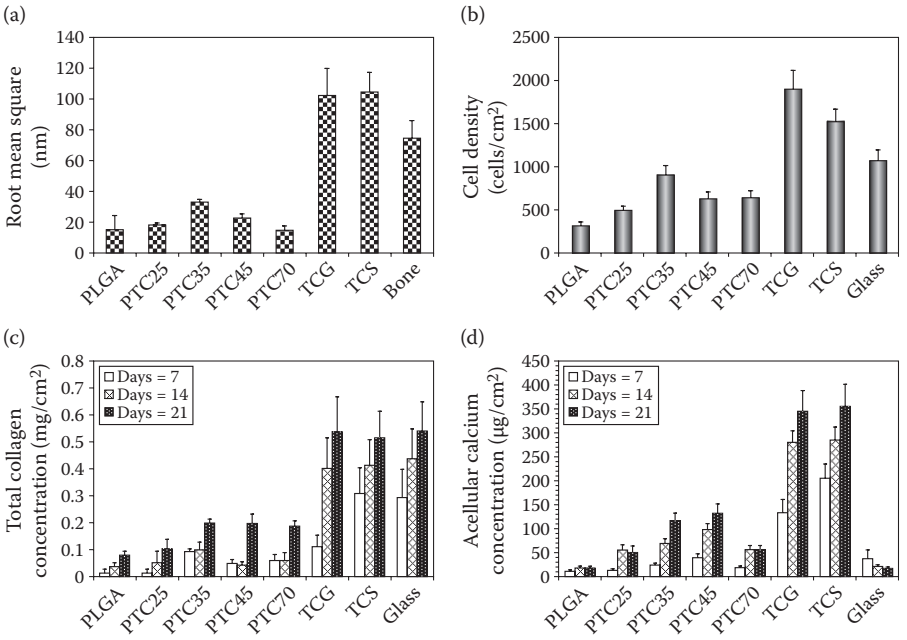

FIGURE 2.8 (a) Surface roughness (root mean square) of PLGA, nanoparticulate titania–PLGA (ultrasonicated at 25%, 35%, 45%, and 70% maximum power), green titania (TCG), sintered titania (TCS), and porcine bone. (b) Cell adhesion to various materials [PLGA, nanoparticulate titania–PLGA (ultrasonicated at 25%, 35%, 45%, and 70% maximum power), TCG, TCS, and glass] after incubation for 4 h. (c) and (d) Total collagen content and acellular calcium concentration for various surfaces analyzed. (From Liu, H. et al., Increased osteoblast functions among nanophase titania/poly(lactide-co-glycolide) composites of the highest nanometer surface roughness, *Journal of Biomedical Materials Research, Part A*, 78, 798, 2006. Reproduced with permission from Wiley.)

Further biological considerations of PMNC performance include fibroblast activity, because excessive fibrosis at the implant–host interface is a known factor in device failure (Vance et al. 2004). Prolonged increased fibroblast numbers at implant interfaces is associated with callous formation and associated soft-tissue formation rather than bone juxtaposition. Thus, a reduction in fibroblast activity (or limited increase in fibroblast activity relative to osteoblasts) might be beneficial to device-mediated wound healing. Promisingly, some studies have shown that the ratio of osteoblast to fibroblast adhesion increased from 1:1 on microparticle alumina surfaces to 3:1 on nanoparticle surfaces (Vance et al. 2004).

Qualitative arguments for the improvement in biological action of nanostructured materials assumed that the improvement was due to mimicking the naturally occurring topographies of natural biological tissues; HA crystals in bone are approximately 50 nm long and 5 nm in diameter. More quantitatively, the enhanced bioactivity observed with nanocomposites results from protein interactions with nanopatterned surfaces (Christenson et al. 2006), whereby cumulative protein absorption has been

shown in many studies to be higher on nanograined materials (Webster et al. 1999, 2000a, 2000b). Several proteins that are known to augment osteoblast function have been shown to be deposited much faster and in greater quantity on nanocomposites compared to microcomposites. Dimensionality effects are also observed in cartilage and tendon tissue engineering constructs. Research indicates that chondrocyte and mesenchymal stem cell activities are strongly dependent on scaffold dimensionality (Lu et al. 2002).

Nanoparticulate addition to composites and surface coatings is not the only application of nanotechnology to medical devices. Other techniques have been used to create nano-sized surface features via chemical etching, electron beam lithography, and polymer demixing (Schift et al. 2002; Thapa et al. 2003), and nanopatterned surfaces produced by electrospraying, which has demonstrated the ability to direct osteoblast growth (Thian et al. 2008).

2.4 THEORETICAL APPROACH

There has been significant development of mathematical models designed to predict the rate of drug release from pure biopolymers using a variety of modeling techniques, many of which elucidate the observed phenomena to a high degree of accuracy for materials with simple geometries such as planes, cylinders, and spheres. However, modeling descriptions of PMNC behavior and degradation kinetics are underdeveloped due to the complexity of degradation processes. Many polymer degradation models employing a plethora of techniques, ranging from Monte Carlo statistical analyses of PLGA microspheres to direct analytical solutions of Fick's equations, have been described in the literature. Finite element modeling is now being used as an indispensable modeling tool, and models have been developed to predict degradation mechanics and diffusion mechanisms in pure polymer matrices. Pan et al. (2011) have advanced model complexity to include the effects of ceramic incorporation. For simplicity, the degradation model of TCP–PLGA composites assumes abundant water absorption and a spherical representative unit volume of a TCP particle surrounded by a PLGA matrix. PLGA degradation is primarily a chain end scission. Wang et al. (2008), Han and Pan (2009), and Han et al. (2010) showed that the rate of chain scission $\frac{dR}{dt}$ is equal to

$$\frac{dR}{dt} = \frac{dC_{end}}{dt} = k_1 C_e + k_2 C_e C_{H^+} \tag{2.9}$$

where C_e, C_{H^+}, k_1, and k_2 represent the ester concentration, hydrogen ion concentration, random polymer scission rate (uncatalyzed reaction), and autocatalysis rate constants, respectively. The concentrations of the ions at each step are calculated by dissociation rate constants. Moreover, the model must account for the differing solubilities of the calcium phosphates. Equilibrium in Equation 2.3 is not reached due to removal of phosphate ions via processes in Equations 2.4 through 2.6. Accordingly, there is an undersaturation leading to TCP dissolution. The rate of TCP dissociation may be described in terms of an ion flux J, which depends on the surface area of the